GOTHENBURG UNIVERSITY

MASTER THESIS, 60 HEC

Ash distribution and cavities in Icelandic glaciers, a marker for snow accumulation and radar signal velocity change

---

Author:
Andrea Håkansson

Supervisor:
Professor Erik Sturkell and
Professor Guðfinna
Aðalgeirsdóttir

A thesis submitted in fulfillment of the requirements
for the degree of Master of Science

at the

Department of Earth Science

September 21, 2019

ABSTRACT

Glaciers in the geologically active Iceland has a high scientific as well as touristic value. In this thesis, the two largest glaciers on Iceland have been studied with GPR to find if the method is suitable to use in future glaciolocial studies where accumulation patterns and similar attributes are in focus in a world of deglaciation. The studies at Langjökull were performed over a manmade icetunnel, and the studies at Vatnajökull were done at Háabunga, where a meter-thick ash-layer was deposited in 2011. At Langjökull the results were good enough to say that the method is suitable to find tunnels and crevasses with GPR, and the GPR measurements together with a CMP measurement at Háabunga yielded an accumulation pattern model with correct depths to the ashlayer, depth ranging from 10.2–17.5 m. This makes it an excellent tool for glacier studies.

Key words: *ICELAND*, *GPR*, *CMP*, *GLACIER*, *VATNAJÖKULL*, *HÁABUNGA*, *LANGJÖKULL*

SAMMANFATTNING

Glaciärer på det geologiskt aktiva Island har ett högt vetenskapligt värde liksom turistiskt värde. I denna uppsats har de två största glaciärerna på Island undersökts med markradar, GPR, för att se om metoden är lämplig för glaciologiska studier där ackumulationsmönster och andra attribut är i fokus i en värld där glaciärer försvinner. Undersökningarna på Langjökull utfördes ovan en människotillverkad istunnel och undersökningarna på Vatnajökull utfördes på Háabunga där ett metertjockt asklager deponerades år 2011. Resultaten från Langjökull visade att metoden är lämplig för att hitta både tunnlar och naturliga sprickor, GPR-mätningarna på Háabunga, tillsammans med CMP-undersökningar gav en ackumulationsmönstermodell som visar ett korrekt djup ned till asklagret, ett djup som varierar från 10,2–17,5 m. Detta gör markradarn till ett utmärkt verktyg för att studera glaciärer.

Nyckelord: *ISLAND*, *MARKRADAR*, *CMP*, *GLACIÄR*, *VATNAJÖKULL*, *HÀABUNGA*, *LANGJÖKULL*

Acknowledgements

First and foremost I would like to thank my supervisors, Professor Erik Sturkell and Professor Guðfinna Aðalgeirsdóttir, for endless support and encouragement. I would also like extend a thank you to the University of Iceland and the Icelandic Glaciological Society (JÖRFI) for bringing me up on these beautiful glaciers, and to Erik Sturkell and Gabrielle Stockmann for housing me on my two months on Iceland. To my examiner, Mats Olvmo, thank you for your constructive criticism which made this manuscript better, and for your understanding and encouraging words when data was lost.

For all help with practicalities during the expeditions I would like to thank Finnur, Eyólfur, and all others that have helped me with my equipment and lending me theirs. I would also like to thank *Into the Glacier* for generously allowing me to use their data.

And in the end, my family and friends that have supported me during these years – thank you!

Table of Contents

Abstract **i**

Acknowledgements **ii**

Table of Contents **iii**

1 Introduction **1**
1.1 Background 1
1.2 Aim 1
1.3 Geological setting 2
1.3.1 Iceland 2
1.3.2 Icelandic glaciers 3
Langjökull 4
Vatnajökull 4
1.3.3 The Ice tunnel 4
1.3.4 Ash layers in glaciers 4

2 Method **7**
2.1 Ground Penetrating Radar (GPR) 7
2.1.1 Scientific background, GPR 7
2.1.2 GPR-setup 7
2.1.3 Rough Terrain Antenna, RTA 9
2.1.4 Common Mid Point, CMP 9
2.1.5 GPS 10
GPS data 10
2.2 Reflex W 10
2.3 Processing and modelling of data 12
2.4 Datasets 12
2.4.1 GPS 12
2.4.2 Level data, ice tunnel 12

3 Langjökull **13**
3.1 Results . . . 13
3.1.1 GPR-profiles . . . 13
3.1.2 Models . . . 13
3.2 Discussion . . . 13

4 Vatnajökull **17**
4.1 Results . . . 17
4.1.1 CMP . . . 18
4.1.2 GPR-profiles . . . 19
Háabunga . . . 19
4.1.3 Models . . . 19
4.2 Discussion . . . 19
Háabunga . . . 19

5 Conclusions **25**
5.1 Langjökull . . . 25
5.2 Vatnajökull . . . 26

References **27**

A Detailed GPR methods **29**
A.1 GPR method . . . 29
A.2 CMP . . . 30

B Seismic Reflection Analyst Tutorial **32**

List of Figures

1.1 Satellite image of Iceland with locations marked with orange. a) Langjökull and b) the area around the volcano Grímsvötn at Vatnajökull, including Háabunga which is marked with a red circle. Image produced by NASA. CC-by-2.5 3
1.2 Ash deposits on Vatnajökull/Háabunga from the 2011 eruption of the volcano Grímsvötn. Photo by Erik Sturkell. 5
1.3 Ashlayers in the glacier ice of the melting part of Langjökull. Photo by Erik Sturkell. 6

2.1 Control unit and monitor for the Malå/RAMAC CUII system 8
2.2 The GPR setup, here at Langjökull 9
2.3 Workflow in software ReflexW 11

3.1 Location of A and B profiles over the tunnel as it was in 2015 14
3.2 Processed GPR profiles at Langjökull, profiles A and B. 15
3.3 Hyperbola in the beginning of Langjökull profile B. 16
3.4 Tunnel depth as modeled in GIS 16

4.1 The profiles in the way they related to each other, and in which direction they were measured. 17
4.2 Analysing the CMP data from Háabunga in ReflexW 18
4.3 Processed GPR profiles at Háabunga, profiles E01–E02 and E03–E04. Ash layer marked with arrows 21
4.4 Processed GPR profiles at Háabunga, profiles E05–E06 and E07–E08. Ash layer marked with arrows 22
4.5 Processed GPR profiles at Háabunga, profiles E09–E10 and E11–E12. Ash layer marked with arrows 23
4.6 Depth to the ashlayer at Háabunga, modeled with coloured fields (left) and isolines (right). 24

A.1 How a hyperbola forms from a void or an item in GPR data. Figure courtesy by Professor Erik Sturkell. 30

A.2 CMP-setup that illustrates the moveout by Nx from a common mid point. Figure courtesy by Professor Erik Sturkell. 31

List of Abbreviations

GPR	**G**round **P**enetrating **R**adar
CMP	**C**ommon **M**id **P**oint
RTA	**R**ough **T**errain **A**ntenna
MHz	**M**ega **H**er**z**
LGM	**L**ast **G**lacial **M**aximum
LIA	**L**ittle **I**ce **A**ge
ELA	**E**quilibrium **L**ine **A**ltitude
m a.s.l.	**m**eters **a**bove **s**ea **l**evel
RMS	**R**oot **M**ean **S**quare
TWTT	**T**wo **W**ay **T**ravel **T**ime
BP	**B**efore **P**resent
AD	**A**nno **D**omini
Ma	**M**ega **a**nnum
ka	**k**ilo **a**nnum
IDW	**I**nverse **D**istance **W**eighting

1 Introduction

1.1 Background

GPR is a great tool for looking into the sub surface, in order to see what lies beneath the surface, without the need to dig into the ground. This makes it valuable for operations where it is imperative that the ground is not disturbed in any way, e.g. archaeological digs or when the area to cover is too big to be able to survey with field-geotechnichal methods such as drilling.

The results of a GPR survey yield an image which can be interpreted by finding reflectors that are caused by the different layers in the sub surface. Knowing the velocities of which the signal travels through the different media is key to interpret these results, since the velocity is needed to find the thickness of the medium, and for glacier ice it is hard to easily find these velocities. Today, most companies and GPR-users have standard velocities for different media, but since nature is inconsistent, and the behaviour of a sand differs from area to area, these standard velocities are not yielding exact results in terms of layer thicknesses and therefor also interpretation.

Langjökull on Iceland is a glacier with high touristic value, as well as scientific, both for the same reason. In 2015, a cave was dug out of the glacier ice for tourists to visit. This gives a unique opportunity for GPR-studies, since the cave is known in both shape in size, measurements here could give the sought-after velocities as well as finding out how a void of known size is represented in GPR.

Using the velocities found, and calibrating after that, it is then possible to apply this to the area around Grímsvötn, a caldera at Iceland's biggest glacier, Vatnajökull. It is of scientific interest to find the accumulation of ice in the area, this can be done using ash layers in the ice from known volcanic events, like the 2011 eruption of Grímsvötn which left thick ash layers at an area called Háabunga, that can be seen as clear reflectors in the GPR results.

1.2 Aim

The goal with this thesis is to find wheter the GPR method is suitable for studying features within glaciers in locations situated above the ELA. The aim for this study is thus

to find signal velocities for GPR in glacier ice at Langjökull and Háabunga, Vatnajökull, and then use these findings to measure and interpret radar signal velocity changes and ice accumulation variations at Háabunga. This will be done by GPR profiling at several glacier locations around Iceland, and the suitability of the method will in the end be discussed.

The study will try to meet the aim with the help of the following research questions, divided by the different localities. For Langjökull these questions are;

- Can we see the Langjökull ice tunnel with the radar, and how does that signal change with depth?
- If so, can we use that information for radar velocity determination?
- Is it possible to determine whether the void signal comes from natural cavities (i.e. crevasses) or anthropogenic cavities (i.e. the tunnel)?

GPR measurements as well as a CMP analysis will be done at Vatnajökull, on the area that is called Háabunga, with the following questions in mind;

- Can the method find the ash layer, and if so also measure the correct depth to it?
- Is there a variation of snow accumulation, and can that be determined with the GPR?
- Can the 2011 ash-layer be found with CMP?

These research questions will bring a further understanding to how the method of GPR on glaciers can be utilised, and how it might be a valuable tool for future glaciological studies.

1.3 Geological setting

1.3.1 Iceland

Iceland is geologically a very active area, with active volcanism and seismic activity. This is because the country is not only situated on a volcanic hotspot, but also in the middle of the Atlantic Mid-Ocean Ridge which splits the island in two parts (Ingolfsson et al., 2008; Bjarnason, 2008). The eastern- and westernmost parts of Iceland are the oldest – up to 16 Ma and the middle of the island is the youngest with active spreading zones (Harðarson, Fitton, and Hjartarson, 2008). The island is comprised to over 80% of basalt (Gíslason, 2008).

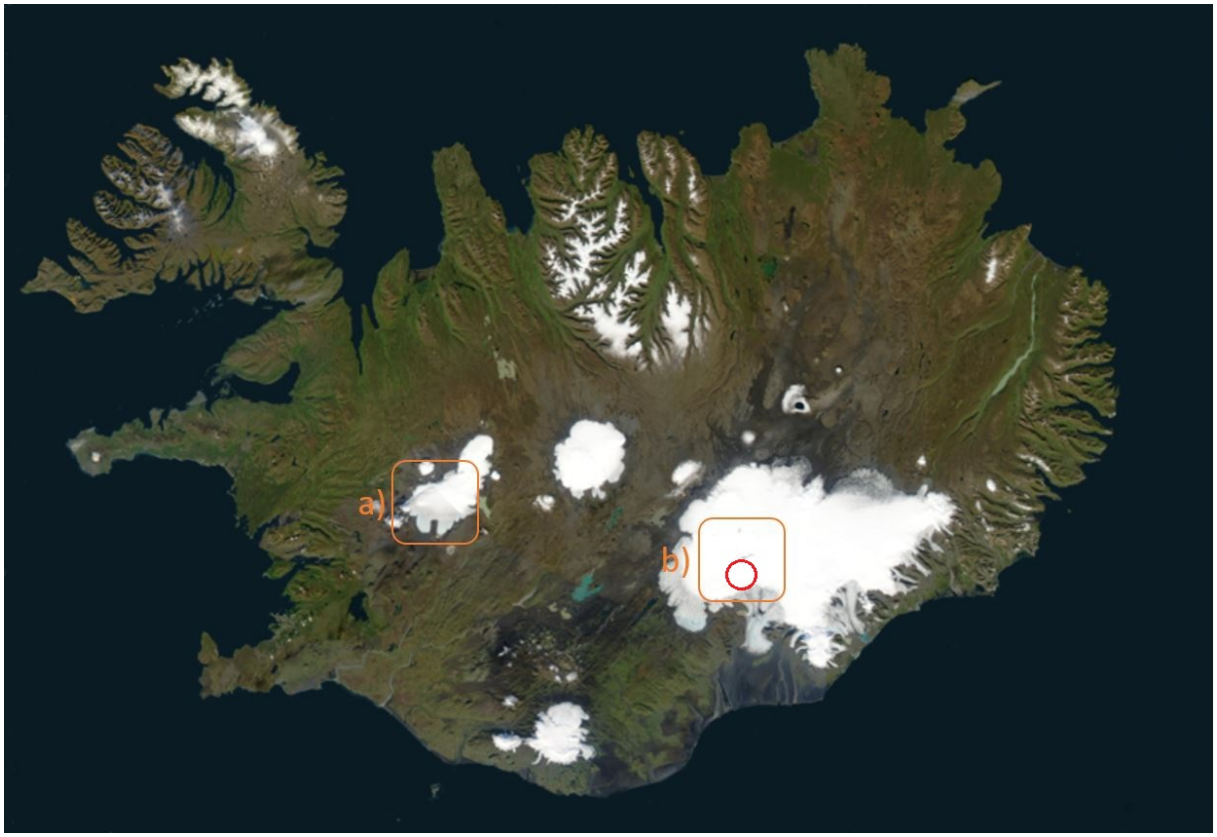

FIGURE 1.1: Satellite image of Iceland with locations marked with orange. a) Langjökull and b) the area around the volcano Grímsvötn at Vatnajökull, including Háabunga which is marked with a red circle. Image produced by NASA. CC-by-2.5
, and modified by the author.

1.3.2 Icelandic glaciers

There are several glaciers on Iceland, as the name suggests, and the work in this thesis is concentrated to the two largest of the Icelandic glaciers – Vatnajökull and Langjökull (figure 1.1). These are also the largest in Europe. As it is, 10% of Iceland's mainland is covered by ice, which makes it a very distinct feature of the country. The Icelandic glaciers are classified as temperate (or warmbased), and they respond quickly to fluctuations in climate (Björnsson and Pálsson, 2008).

During the last 2.5 Ma, there are sedimentological evidence for a minimum of 20 major glaciations where the whole country was covered by ice, many of which are preserved due to lava flows covering the glacial sediments (Ingolfsson et al., 2008).

Iceland's late Weichselian and Holocene glaciation history has the same general story as the rest of the northen hemisphere. The LGM occured circa 20 ka BP where the ice sheet covered the whole of Iceland as well as tens of kilometers off shore. It has been calculated that the thickness of the ice sheet was around 1500 meter over the central highlands of Iceland. The ice sheet then retreated during the period following,

but increased again to almost cover the whole island during Younger Dryas (12.9–11.7 ka). Then they retreated again to a state at around 8 ka BP where some of the ice caps existing today were either the same size as in the present, or even non-existent. At about 6–5 ka BP, neoglaciation started, and this late-Holocene glaciation seems to have had its last maximum extent during LIA (Norðdahl et al., 2008). Since that time the glaciers have steadily retreaded, and today they are doing so very rapidly, as is the case in the rest of the world.

Langjökull

Langjökull (see A in figure 1.1) is, with its 925 km^2, the second largest glacier on Iceland and has a volume of 190 km^3(Björnsson and Pálsson, 2008; Pope et al., 2016). It also houses the touristically valued "Ice Tunnel", which will be described further down.

Vatnajökull

Vatnajökull (see B in figure 1.1) is the largest ice cap in Europe (the largest in *continental Europe* being Jostedalsbreen in Norway) with an area of 8100 km^2 and a volume of 3100 km^3 (Björnsson and Pálsson, 2008). Háabunga (the word *bunga* loosely translates to *bulge*) is a hill area just south of the volcano Grímsvötn (see red circle in figure 1.1), on which ash from a volcanic eruption of Grímsvötn in 2011 was deposited (read more in section 1.3.4 Ash layers in glaciers). Grímsvötn, being one of the many volcanoes hidden beneath the cover of Vatnajökull, could have had as many as 30 eruptions during the last 400 years, and the latest was in 2014 (Björnsson, 2003; Björnsson and Pálsson, 2008).

1.3.3 The Ice tunnel

The ice tunnel in Langjökull was created in 2010 by a team of engineers, a tourist company, and... The tunnel reaches 140 meters inside the glacier and is situated close to the ELA. It starts as one tunnel, that later divides into two, which then goes around to form almost a heart shape. The tunnel also features several rooms, such as a chapel, lecture room, and the whole thing is cut by a crevasse that goes through the eastern part of the tunnel, running from north to south (*What is Into the Glacier?* 2016).

1.3.4 Ash layers in glaciers

Icelandic volcanoes have several ways of erupting. It could erupt on land, under water, or under ice (Ingolfsson et al., 2008). A felsic magma often produces more ash than a mafic magma, since a felsic volcanic eruption is more likely to be explosive, but as

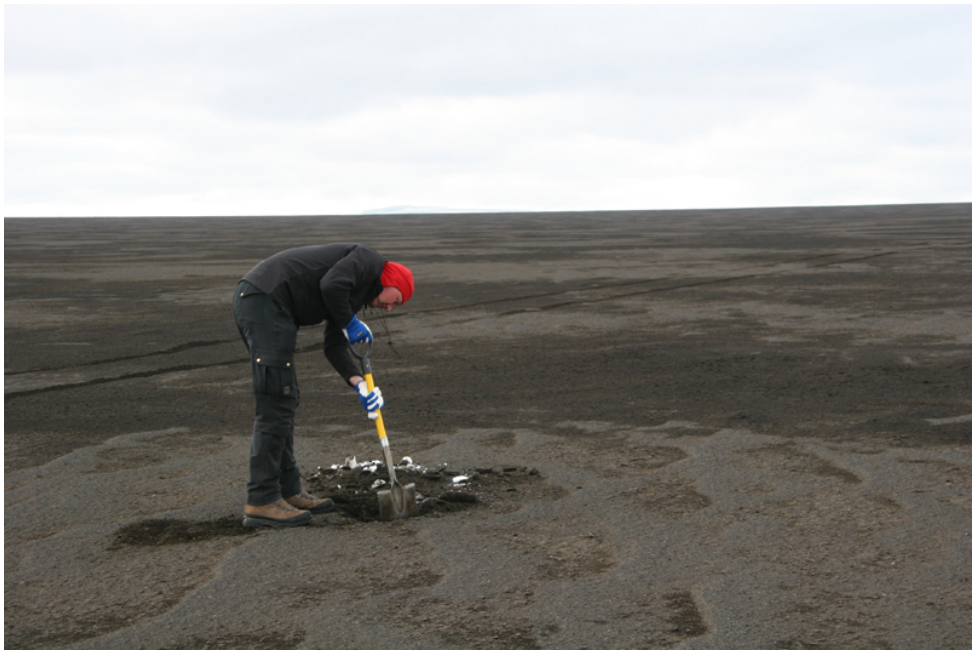

FIGURE 1.2: Ash deposits on Vatnajökull/Háabunga from the 2011 eruption of the volcano Grímsvötn. Photo by Erik Sturkell.

stated, on Iceland there is also the possibility of subaqueaus or subglacial eruptions, where the added volatiles can produce the explosiveness needed for ash release even in basaltic magmatic systems (Larsen and Eiríksson, 2008; Ingolfsson et al., 2008).

Grímsvötn, being one of the six mafic volcanic systems that produce the most ash on Iceland, have had at least 60 eruptions since the year 1300 AD (Jakobsson and Gudmundsson, 2008; Larsen and Eiríksson, 2008; Björnsson, 2003) and the latest was in 2014. Wind and other causes deposited the ash from the 2011 eruption directly south of the caldera on the part of Vatnajökull that is called Háabunga (see red circle in figure 1.1. The thickness of that ash-layer (seen in figure 1.2) is over a meter (Sturkell 2019, personal communication). These ash-layers will then be buried when snow later accumulates on the glacier, and will at the end form layers in the glacier sequence (see figure 1.3).

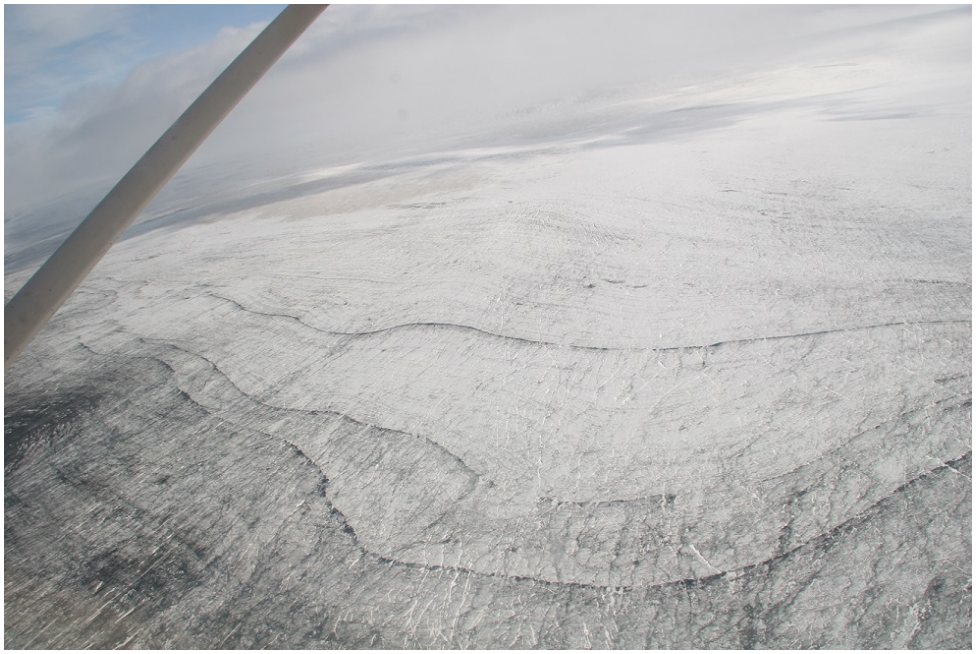

FIGURE 1.3: Ashlayers in the glacier ice of the melting part of Langjökull. Photo by Erik Sturkell.

2 Method

2.1 Ground Penetrating Radar (GPR)

2.1.1 Scientific background, GPR

The way the GPR method is working is through sending out electromagnetic signals through a transmitting antenna, which then are reflected from different layers and items in the subsurface if they have a different relative permittivity. These reflected signals are then taken up by the receiving antenna, amplified, and sent to the control unit of the system. The distance is measured in TWTT, which then can be translated to depth in meters (Degenhardt Jr, 2009; Monnier et al., 2011; Mussett and Khan, 2000).

The antenna frequency plays a role in the resolution of the data – the higher the frequency the higher the resolution. This is due to layers that are closer together than the distance of circa half a wavelenght can not be separated in the resulting data (i.e. two layers/reflectors that are closer together than half the wavelenght of the antenna used will not be visible as two separate layers in the resulting radargram, but rather as one). The opposite is true for penetration depth. A lower frequency yields a deeper penetration since the amplitude of the wave decreases exponentially for every travelled wavelenght, which means that a higher frequency wave will get absorbed much faster than a lower frequency wave (Mussett and Khan, 2000).

Depending on the relative permittivity of the material, ε_r, the signal travels with different velocity, and it is this velocity that is used to translate the TWTT to depth in meters at the processing stage (BurVal, 2006). These differences in material can be seen in Table 2.1. For a more detailed description of the method, see Appendix B.

2.1.2 GPR-setup

A Malå RAMAC/GPR CUII control unit with a XV monitor was used together with a RTA 50 MHz antenna. This was mounted on a sled behind a snowmobile, on which a GPS antenna was set up, see figures 2.1 and 2.2.

TABLE 2.1: Properties observed for different medium at 100 MHz. Table after Davis and Annan, 1989

Material	**Relative permittivity** ε_r	**Velocity** $V\ (m\ ns^{-}1)$	**Electrical conductivity** $\sigma\ (mS\ m^{-}1)$
Air	1	0.3	0
Fresh water	81	0.033	0.5
Ice (pure)	3 – 4	0.16	0.01
Sand (dry)	3 – 5	0.15	0.01
Sand (wet)	20 – 30	0.6	0.01 – 1

FIGURE 2.1: Control unit and monitor for the Malå/RAMAC CUII system

FIGURE 2.2: The GPR setup, here at Langjökull

2.1.3 Rough Terrain Antenna, RTA

A RTA with a centre frequency of 50 MHz with an antenna spacing of 4 meter was used for the profiles. This allows for a deeper penetration of the radar into the glacier ice, as well as the possibility of towing the antenna behind a snow-mobile as it is better suited for this than other antennas. The RTA is an un-shielded antenna, which is suitable on glaciers as there are no disturbing elements (e.g. trees or lamp posts) to the sides that can interfere with the signal.

2.1.4 Common Mid Point, CMP

To find a suitable velocity for the ice, a CMP had to be done. CMP-surveys are not done on a normal basis, since standard velocities tend to be most commonly used. This is easier, but yields a result that is not as accurate. Doing a CMP-analysis makes the results more accurate, as it is based on a velocity calculated for the specific location and material.

To peform a CMP-analysis, the two, unshielded, antennae are moved away from eachother with a common mid-point between them. The signal reflects off a horisontal reflector in the subsurface, and the increasing distance the signal travels creates a hyperbola in the radargram, which then is used to calculate the velocity of the signal wave through the subsurface. For a detailed description of the method, see Appendix B.

The CMP was done at Háabunga, on Vatnajökull, right on the profile E05-E06 of the GPR-survey. The configuration for the CMP used a 100 MHz unshielded antenna-set, and they were configured in a PR-BD mode (perpendiular-broadside).

The interval velocities for each layer were automatically calculated within Reflex W, and were then used to for the RMS velocity, which was then calculated using equation 2.1, where v_i is the interval velocity and τ_i is the interval depth in ns. The interval is the different layers in the sequence.

$$V_{rms,n} = \sqrt{\frac{\sum_{i=1}^{n} v_i^2 \tau_i^2}{\sum_{i=1}^{n} \tau_i}} \tag{2.1}$$

2.1.5 GPS

To survey the tunnel on Langjökull and Háabunga on Vatnajökull, a grid pattern was produced as GPS-coordinates. These were then followed in the field. A DGPS (Differential-GPS) with an accuracy of 10 cm was used and the antenna was mounted at the back of the snow mobile, and the data was then provided as an Microsoft Excel-sheet with an exact track of the survey route. These were then processed in ArcMap to produce a track-chart of the survey route.

The profiles were done in one long go, and each turn (sub-profile) was marked with time and radar location for later use.

GPS data

The GPS data was reviewed in GIS and the topographical profile was extracted for every profile to enable the topographic correction of the radar profiles.

2.2 Reflex W

The data from the GPR was then processed in the software Reflex W, following a set of processing steps similar to the ones presented in Carrivick et al., 2007. The filter-operations used to produce the 2D profiles are presented in Figure 2.3.

The last step is the correction for terrain differences, and is done by converting the height from m to ns (2.2), where V is the velocity of the medium in m/ns, t is time in ns, and S is the height in m. As the profiles are shown with relative heights, there is no need for the exact height in m a.s.l, so the relative height difference was used instead, in respect to the lowest point in the profile.

$$t = \frac{S}{V} \tag{2.2}$$

The GPR profiles were processed separately, and after all the processing steps were done, they were divided up as their separate smaller sub-profiles. This was done with the GPS-data together with (if available) start and end data of each sub-profile in the

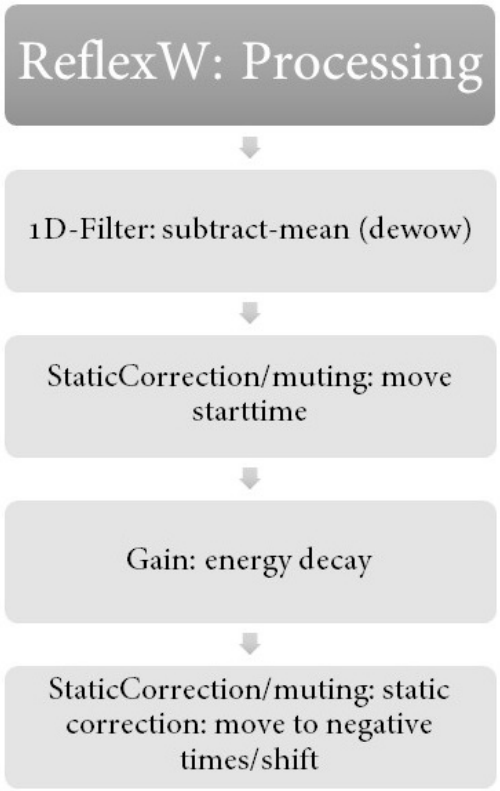

FIGURE 2.3: Workflow in software ReflexW

GPR. If the GPR-distance differed from the GPS, a conversion factor was calculated and used to pinpoint the exact locations of the start and end of the sub-profiles. This was not done for Langjökull, since only the start and end of the whole A and B profiles (see figure 3.1) were registered with regards to GPR distance, but not the sub-profiles. These were then processed separately in the GIS software.

2.3 Processing and modelling of data

The data was then modelled in several softwares (e.g. the ESRI ArcGIS suite, Microsoft Excel, etc.). See Appendix B (Bergstrand and Johansson, 2013) for the GIS-method used to extrapolate the tunnel and ash layers from the different radar profiles.

The tunnel and other clear reflectors were mapped in each profile in ArcMap, which yielded an X, Y, and Z value for each point in the layer. These were then merged together to one file, which was then interpolated with Inverse Distance Weighting (IDW) to form the layer between the profiles. This layer was then plotted in ArcScene to see the tunnel and layer in 3D. The method for mapping the profile layers was done according to B, except that the different profiles were merged instead of exported in step 4.7.

2.4 Datasets

Several datasets were provided by different sources, such as University of Iceland and private companies.

2.4.1 GPS

The GPS data used in the study was extracted and provided by Finnur Pálson at University of Iceland.

2.4.2 Level data, ice tunnel

Level data acquired with laser from inside the tunnel was provided by Into the Glacier, and was provided as .dwg CAD-files. These were reviewed in the software FME Viewer, but could regrettably not be used further due to issues that will be discussed in section 3.2.

3 Langjökull

3.1 Results

3.1.1 GPR-profiles

The final A and B profiles can be seen in figure 3.2. Several hyperbola can be seen throughout both profiles (example enlarged in figure 3.3) as well as several distinct layers close to the surface. At around 270 *ns* depth there is a clear, light layer, that cuts through the hyperbolas in several locations. The difference between the highest and the lowest point in the profiles is around 20 meters.

At some locations, there are even several hyperbola above or in conjunction with each other,

3.1.2 Models

The model in figure 3.4 shows the result of the GIS-mapping of the tunnel/crevasse with depth in *m*. The depth to the tunnel is the greatest towards the top of the figure, in north-east, where it is around 60 *m* and the lowest in the bottom of the picture where it is around 17 *m*. The hyperbolas are marked with points in the figure, and in each profile there are between 1 – 4 mapped hyperbolas.

3.2 Discussion

The tunnel is clearly visible in the data and the results clearly show the importance of being very careful with everything.

The tunnel at Langjökull is clearly visible at several places in the profiles. There are some locations in the profiles where there are several hyperbolas close to each other, and some that are on top of each other. The latter is most likely the tunnel ceiling and tunnel floor that both show up on the radar, whereas the hyperbola close by then could be the crevasse. The radar data with the GIS tunnel mapping is regrettably not possible to correlate with the tunnel in any shape. One could argue that it is because the tunnel location used to produce the coordinates for the two profiles is based on measurements from 2015, and we know that Langjökull moves with a speed of ** at the

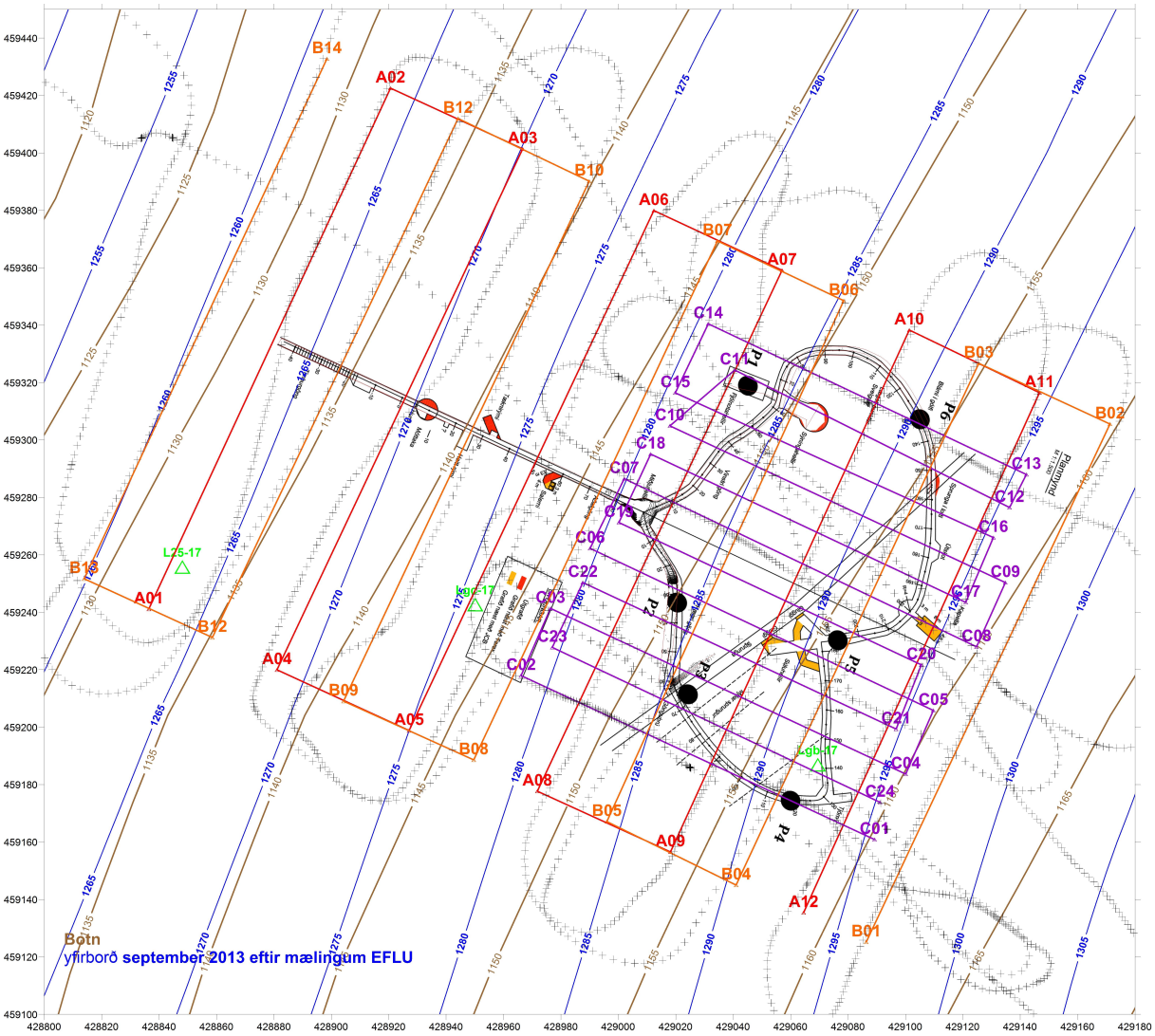

FIGURE 3.1: Location of A and B profiles over the tunnel as it was in 2015

base (citation). This could have made the tunnel disappear from parts of the profiles, but this is most likely not the case. Since the method of correlating the GPS track to the radar distance measuring was not fully developed at the time, the profiles were probably not divided correctly. As a result, the profiles (and therefor also the tunnel and crevasse) have become a bit skewed and shifted with regards to each other. This means that the mapping does not show neither the correct location of that particular tunnel signal nor the correct depth.

Though most of the research questions can be answered, as the tunnel is visible, there are hyperbolas marking both the depth to the tunnel roof and floor. There are also hyperbolas that have a slightly different shape, not as rounded, which then would be the crevasse, but that will not be as easy to tell apart if you do not have both of them to look at the same time.

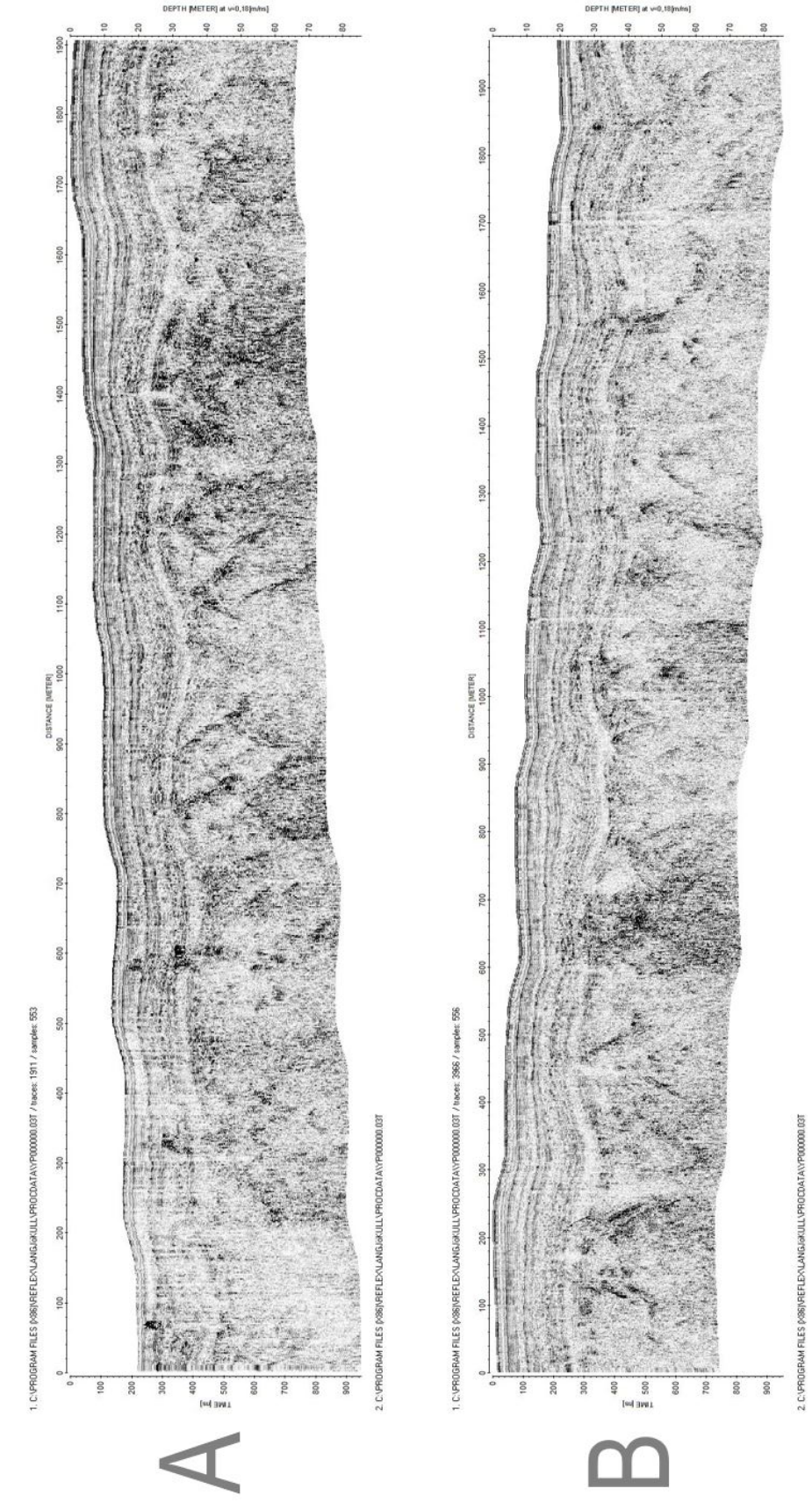

FIGURE 3.2: Processed GPR profiles at Langjökull, profiles *A* and B.

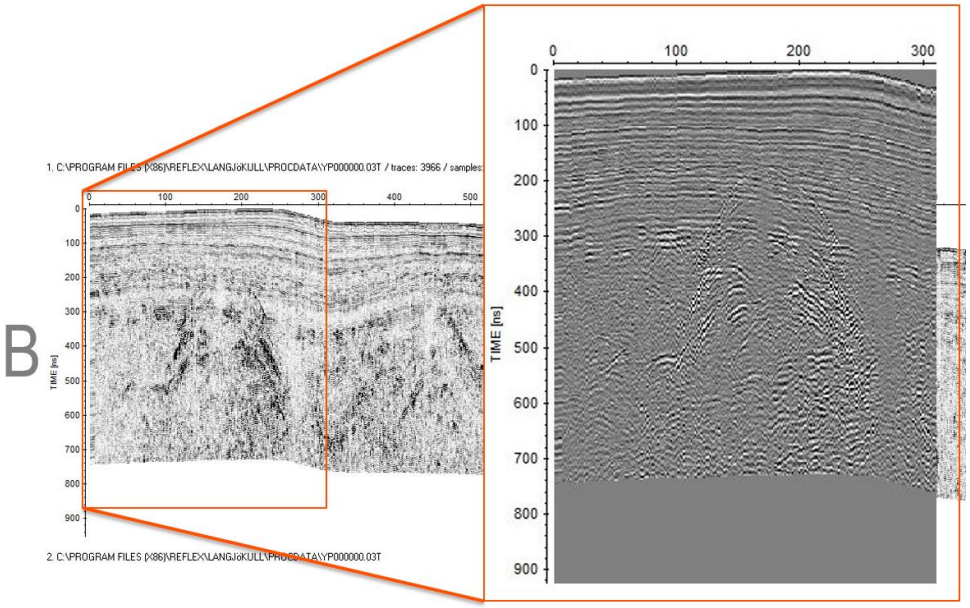

FIGURE 3.3: Hyperbola in the beginning of Langjökull profile B.

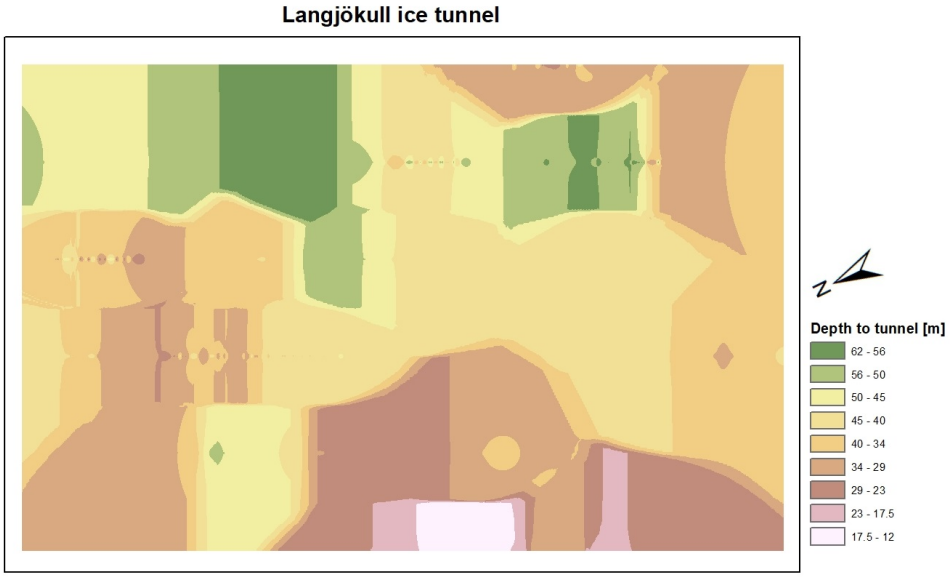

FIGURE 3.4: Tunnel depth as modeled in GIS

4 Vatnajökull

4.1 Results

In this section, the results for the measurements at Háabunga will be presented. The radar profiles were measured according to figure 4.1.

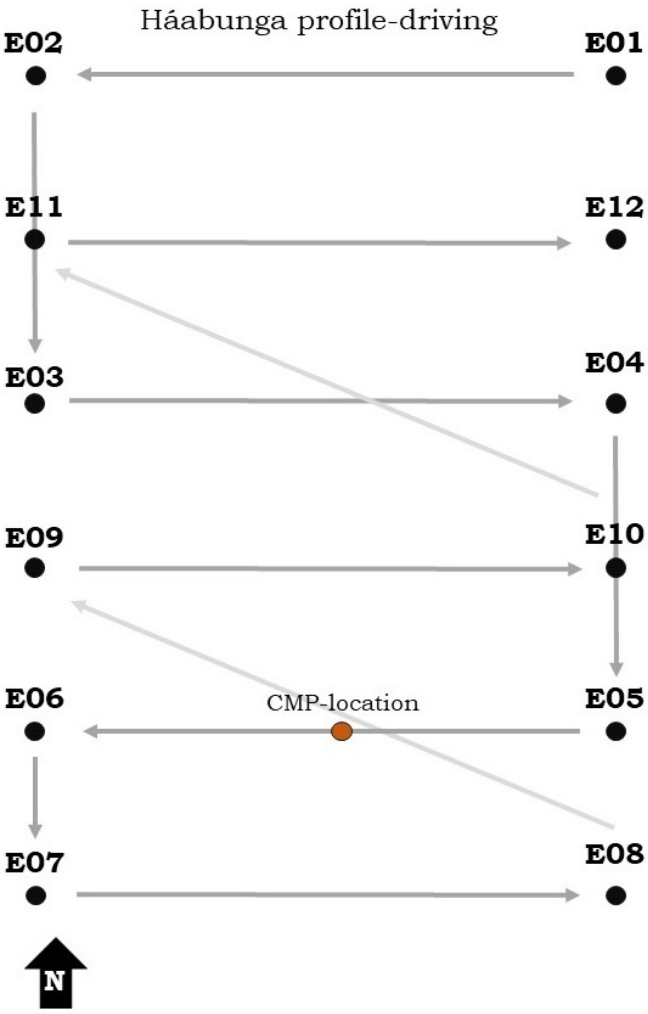

FIGURE 4.1: The profiles in the way they related to each other, and in which direction they were measured.

TABLE 4.1: Layer velocities from CMP-analysis processing in ReflexW

Layer, n	**Velocity** $V\ (m/ns)$	**Thickness** $\tau\ (ns)$	**TWTT** $t\ (m/ns)$
1	0.18267	30	60
2	0.16240	84	144
3	0.22723	140	284

4.1.1 CMP

The CMP-analysis performed at Háabunga and processed in ReflexW (see figure 4.2) yielded three layers with different velocities down to the ash layers. These were of around 0.16 and 0.18 m/ns for the top two layers and 0.22 m/ns for the ice down to the layer at circa 300 ns TWTT. The velocities and other factors that were used in calculating the RMS velocity are found in table 4.1. The RMS velocity was found to be 0.2005 m/ns.

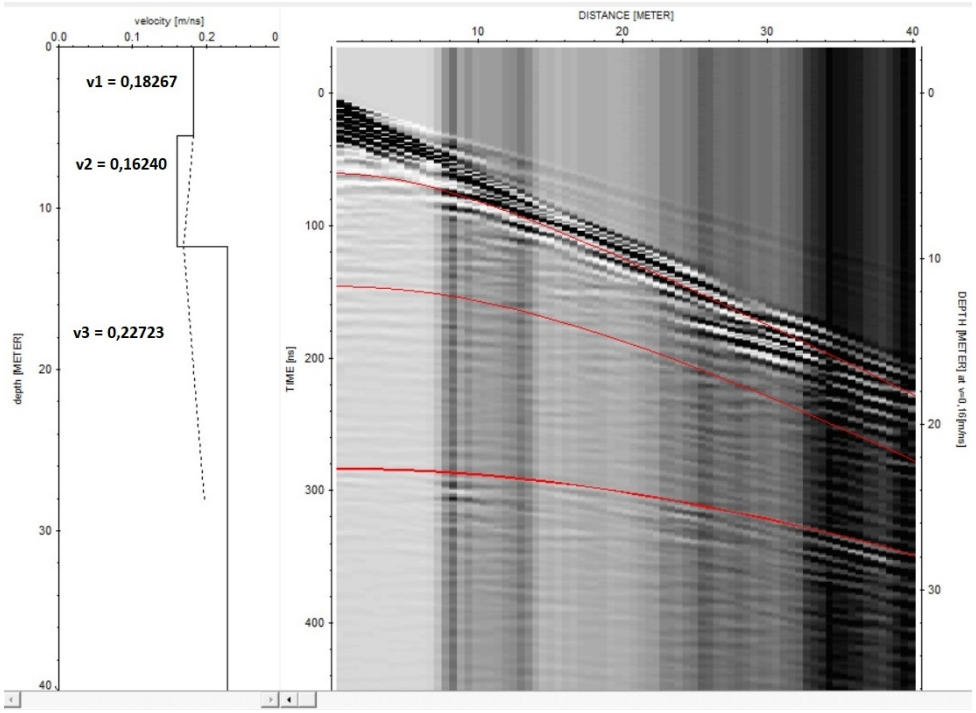

FIGURE 4.2: Analysing the CMP data from Háabunga in ReflexW

4.1.2 GPR-profiles

Háabunga

The different profiles (see figures 4.3, 4.4, and 4.5) from Háabunga show a clear, dark, reflector at circa 300 *ns* depth that continuous through all the profiles. This is the layer that has been interpreted as the ash layer and used as such in the following models. There are also reflectors at the near-surface, parallel to the surface, that gradually disappears by depth.

The surface of the reflector interpreted as the ash layer is somewhat undulating, also where the topography is not.

4.1.3 Models

The depth to the ash layer ranges between 10.2 to 17.5 meters, and the average depth is 13.3 meters. The depth to the as layer is greater in south-west, and the lowest in north-west. This yields a mean annual accumulation of 1.9 m – not accounting for the compaction that takes place as the snow transitions to firn and then finally glacier ice.

4.2 Discussion

Háabunga

The CMP-analyses performed at Háabunga showed velocities of around 0.16 m/ns for the top layers and 0.18 m/ns for the ice down to the ash layer at circa 300 *ns* TWTT. The ash layer it self had a signal velocity of circa 0.22 m/ns. This yield a mean veolocity of 0.20 m/ns for the snow and firn down to the 2011 ash layer. These varying velocities are consistent with the different compaction grades of the snow and firn in a glacier. The transition from firn to ice in a glacier normally happens at depth around 50–120 m, why the sequence has been interpreted as being only snow and firn (Hörhold et al., 2012). The gradual disappearance of clear layers in the radargram would suggest that the transition to glacier happens at a shallower depth than that, but since the antenna frequency is relatively low - 50 MhZ - the layers can very well continue on down in the sequence even though we can not see them, if the layers are thinner than the wavelenght of the signal (see method for more description on the importance of frequency).

Murray, Booth, and Rippin, 2007 made CMP-analyses on the Tsanfleuron glacier in the Alps and on the Bakaninbreen on Svalbard. The RMS-velocities they found ranged between 0.1596–0.1650 m/ns for Tsanfleuron glacier and 0.1662–1725 m/ns on

the Bakanin glacier. This differs from the results from Háabunga because of several reasons. Murray, Booth, and Rippin, 2007 excluded the high-velocity snow layers above the ice from their RMS-velocity, which yields a lower mean, but mostly it depends on the water vs. air content of the glacier. According to their measurements the Tsanfleuron glacier had a water content of 3.9% during the time of their study, whilst the Bakanin glacier had a water content of 1.29% (Murray, Booth, and Rippin, 2007).

The deepest reflector that was used in the CMP-analysis was situated at a depth of about 300 ns, which is the same as the very clear reflector seen in the sub-profile radargrams. This suggest that the RMS velocity calculated in the CMP-analysis is indeed the one down to the ash layer, which validates the certainty of the depth acquired in the GPR-surveying at Háabunga.

The variation of the depth to ash-layer in figure 4.6 shows that the highest accumulation of snow occurs in south-west at Háabunga. The ash-layer generally follows the topography, as would be expected, but the is a substantial difference in accumulation over the area of Háabunga – as much as 7.2 meters in the south-western part of Háabunga.

The undulating surface of the ash layer is most likely due to the uneven melting of the glacier surface, most often caused by wind-blown ash (as is mostly the case on Iceland) or other debris. This debris has a lower albedo than the ice, which causes very localised melting at the glacier surface as the ash and debris take up more heat from the sun, making these undulations in the surface.

Other studies (e.g. Carrivick et al., 2007;Campbell, Affleck, and Sinclair, 2018) that utilises GPR on glaciers rather focuses on finding debris and till structures within the snout of the glaciers, and on the internal structures of land forms produced by glaciers, and the GPR has been considered a good tool for those studies. Comparing the results obtained in this study to them, the extractable data is of similar quality from both Langjökull and Háabunga, though for the former there were other problems than the quality of data that impacted the ability to draw conclusions from it.

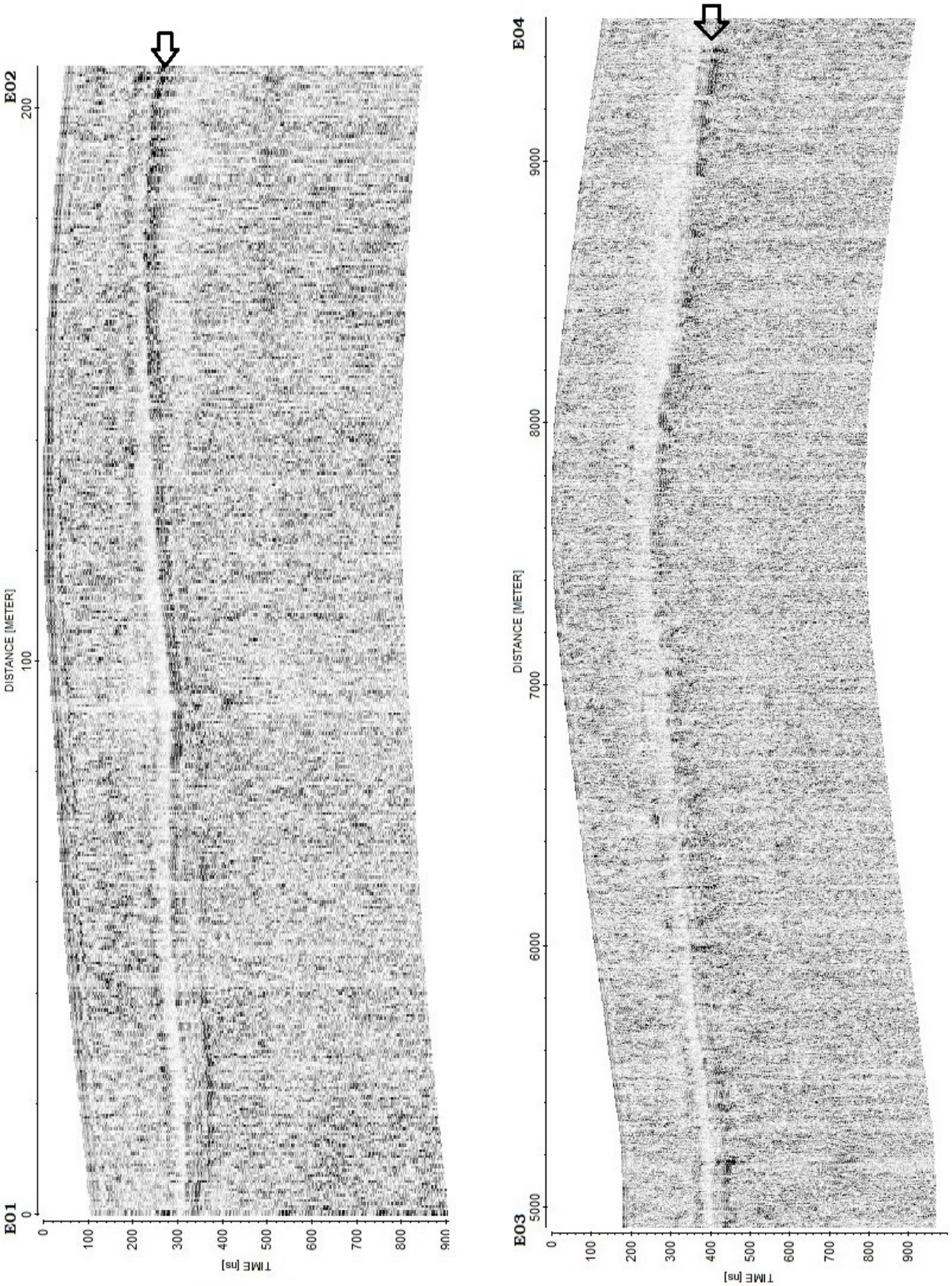

FIGURE 4.3: Processed GPR profiles at Háabunga, profiles E01–E02 and E03–E04. Ash layer marked with arrows

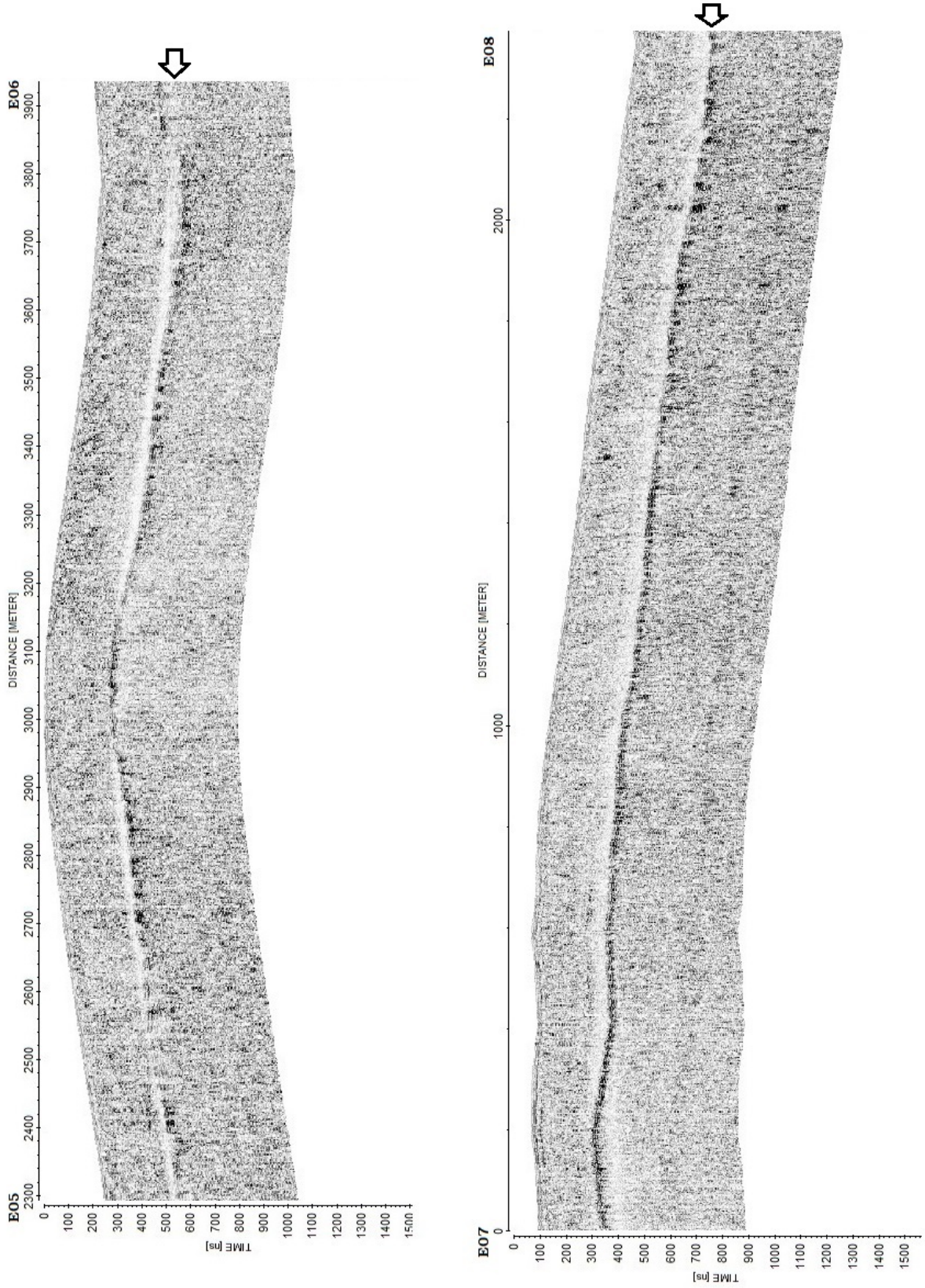

FIGURE 4.4: Processed GPR profiles at Háabunga, profiles E05–E06 and E07–E08. Ash layer marked with arrows

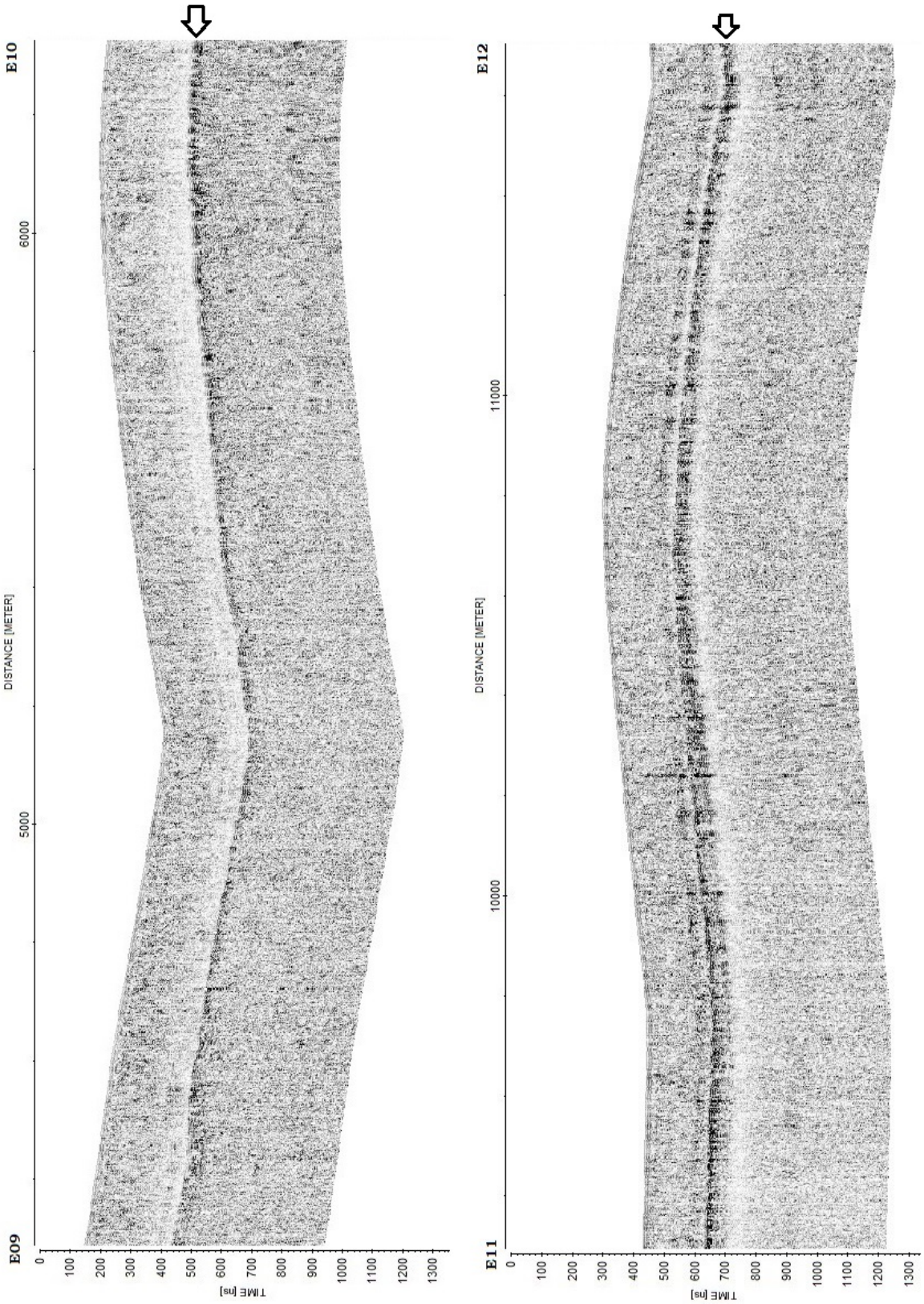

FIGURE 4.5: Processed GPR profiles at Háabunga, profiles E09–E10 and E11–E12. Ash layer marked with arrows

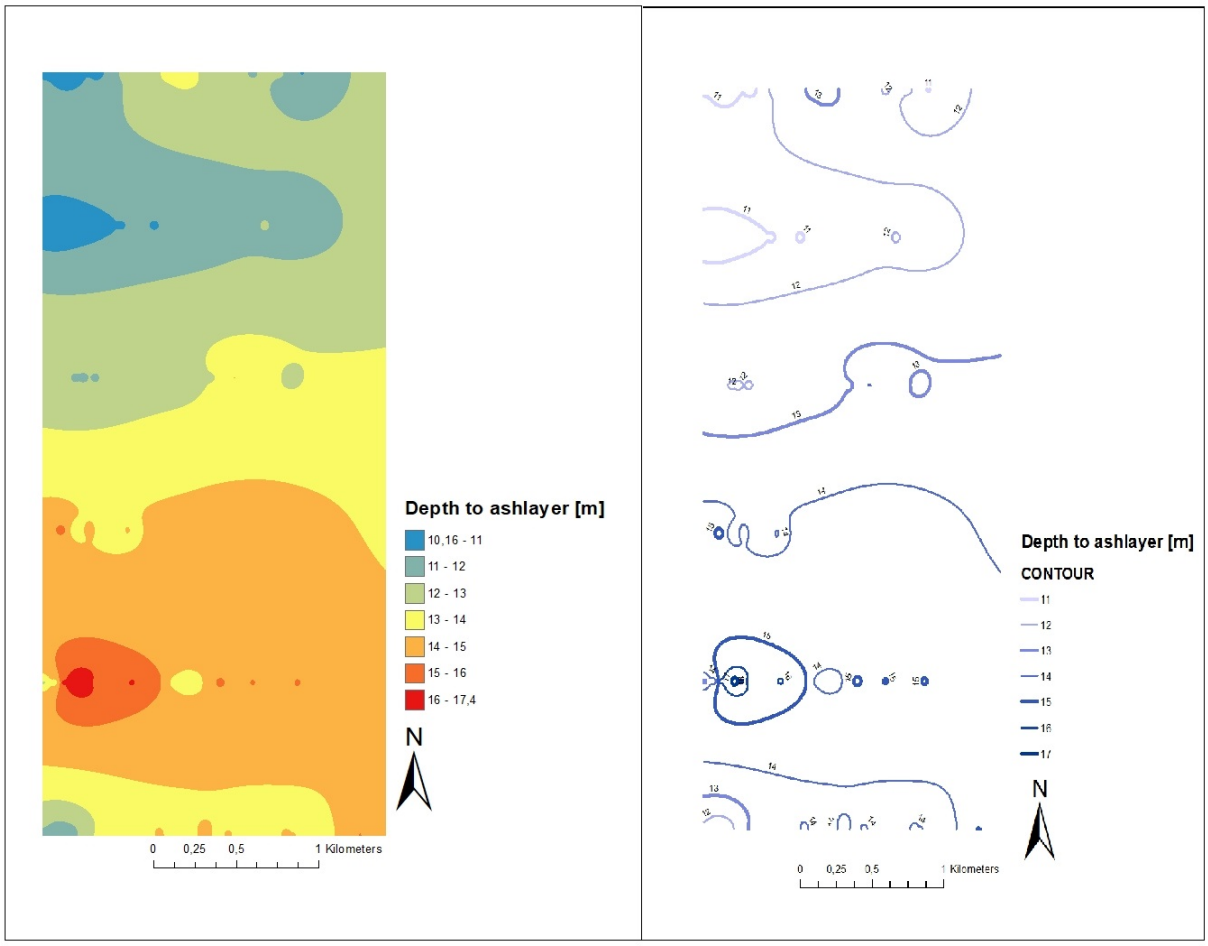

FIGURE 4.6: Depth to the ashlayer at Háabunga, modeled with coloured fields (left) and isolines (right).

5 Conclusions

5.1 Langjökull

The tunnel does indeed show clearly in the radar profiles, and it is possible to locate both depth and position of it from the surface with GPR. There is also a difference between the tunnel and natural crevasses, but it is not possible to tell one from the other if at least one is not known before.

To be able to make an accurate model, one that makes it possible to draw conclusions from it, the errors of the measuring wheel has to be taken into account. Also the horisontal spatial resolution used here (i.e. the sampling interval) is a bit too low to be able to map the tunnel accurately.

Based on the results obtained in this study it can be concluded that;

- The method is suitable to map tunnels in ice.
- Better spatial resolution is needed to perform accurate analysis, as well as careful route planning.

5.2 Vatnajökull

The project must be considered successful at Háabunga, as the targets (i.e. finding the 2011 ash layer, finding the depth of snow and ice to the same layer through measuring the radar velocity with CMP) for the part were met and exceeded. It is indeed suitable to use the GPR at locations like these in future studies. The ash layer appeared as a very distinct reflector in the radargrams, and the lowest hyperbola in the CMP-measurement was at the same depth (i.e. 300 *ns*) as the ash layer in the radargrams from the profiles, which clearly states that the calculated velocity is true and reliable and thus also the modelled depth.

The study also revealed that;

- The ash layer at Háabunga varies in depth.
- The CMP-measurement was successful finding an accurate velocity for the snow and firn layers down to the ash layer and thus the correct depth to the same ash layer.
- Together with suitable glaciological knowledge/science/data, the GPR can be a valueable tool to study snow accumulation on glaciers.

References

Bergstrand, C and J Johansson (2013). "Seismic Reflection Analyst Tutorial". In:

Bjarnason, Ingi Þorleifur et al. (2008). "An Iceland hotspot saga". In: *Jökull* 58, pp. 3–16.

Björnsson, H and F Pálsson (2008). "Icelandic glaciers. Jökull. 58, 365–386". In: *Jökull* 58, pp. 161–178.

Björnsson, Helgi (2003). "Subglacial lakes and jökulhlaups in Iceland". In: *Global and Planetary Change* 35.3-4, pp. 255–271.

BurVal, Working Group et al. (2006). *Groundwater resources in buried valleys: a challenge for geosciences*. GGA-Inst.

Campbell, Seth, Rosa T Affleck, and Samantha Sinclair (2018). "Ground-penetrating radar studies of permafrost, periglacial, and near-surface geology at McMurdo Station, Antarctica". In: *Cold Regions Science and Technology* 148, pp. 38–49.

Carrivick, Jonathan L et al. (2007). "GPR-derived sedimentary architecture and stratigraphy of outburst flood sedimentation within a bedrock valley system, Hraundalur, Iceland". In: *Journal of Environmental & Engineering Geophysics* 12.1, pp. 127–143.

Davis, JL and AP Annan (1989). "Ground-penetrating radar for high-resolution mapping of soil and rock stratigraphy". In: *Geophysical prospecting* 37.5, pp. 531–551.

Degenhardt Jr, John J (2009). "Development of tongue-shaped and multilobate rock glaciers in alpine environments–Interpretations from ground penetrating radar surveys". In: *Geomorphology* 109.3-4, pp. 94–107.

Edward Barrett, Brian, Tavi Murray, and Roger Clark (2007). "Errors in radar CMP velocity estimates due to survey geometry, and their implication for ice water content estimation". In: *Journal of Environmental and Engineering Geophysics* 12.1, pp. 101–111.

Gíslason, Sigurður Reynir (2008). "Weathering in Iceland". In: *Jökull* 58, pp. 387–408.

Harðarson, Björn S, J Godfrey Fitton, and Árni Hjartarson (2008). "Tertiary volcanism in Iceland". In: *Jökull* 58, pp. 161–178.

Hörhold, MW et al. (2012). "On the impact of impurities on the densification of polar firn". In: *Earth and Planetary Science Letters* 325, pp. 93–99.

Ingolfsson, Olafur et al. (2008). "The dynamic geology of Iceland". In: *Jökull* 58, pp. 1–2.

Jacob, Robert W and TM Urban (2016). "Ground-Penetrating Radar Velocity Determination and Precision Estimates Using Common-Midpoint (CMP) Collection with

Hand-Picking, Semblance Analysis and Cross-Correlation Analysis: A Case Study and Tutorial for Archaeologists". In: *Archaeometry* 58.6, pp. 987–1002.

Jakobsson, Sveinn P and Magnús T Gudmundsson (2008). "Subglacial and intraglacial volcanic formations in Iceland". In: *Jökull* 58, pp. 179–196.

Larsen, Guðrún and Jón Eiríksson (2008). "Holocene tephra archives and tephrochronology in Iceland–a brief overview". In: *Jökull* 58.2005, pp. 229–250.

Monnier, Sébastien et al. (2011). "Structure and genesis of the Thabor rock glacier (Northern French Alps) determined from morphological and ground-penetrating radar surveys". In: *Geomorphology* 134.3-4, pp. 269–279.

Murray, Tavi, Adam Booth, and David M Rippin (2007). "Water-content of glacier-ice: Limitations on estimates from velocity analysis of surface ground-penetrating radar surveys". In: *Journal of Environmental & Engineering Geophysics* 12.1, pp. 87–99.

Mussett, Alan E and M Aftab Khan (2000). *Looking into the earth: an introduction to geological geophysics*. Cambridge University Press.

Norðdahl, Hreggviður et al. (2008). "Late Weichselian and Holocene environmental history of Iceland". In: *Jökull* 58, pp. 343–364.

Pope, Ed L et al. (2016). "Contrasting snow and ice albedos derived from MODIS, Landsat ETM+ and airborne data from Langjökull, Iceland". In: *Remote Sensing of Environment* 175, pp. 183–195.

What is Into the Glacier? (2016). `https://intotheglacier.is/about/`. Accessed: 2018-05-22.

A Detailed GPR methods

A.1 GPR method

The way the GPR method is working is through sending out electromagnetic signals through a transmitting antenna, which then are reflected from different layers and items in the subsurface if they have a different relative permittivity. These reflected signals are then taken up by the receiving antenna, amplified, and sent to the control unit of the system (Degenhardt Jr, 2009; Monnier et al., 2011). The antenna frequency plays a role in the resolution of the data - the higher the frequency the higher the resolution, but the opposite is true for penetration depth. A lower frequency yields a deeper penetration.

Relation between frequency and resolution, and depth seeing. Central operating frequency. Setup behind snowmobile and a sled Depending on the relative permittivity, ε, the signal travels with different velocity. These differences in material can be seen in Table 2.1.

To calculate the velocity and depth, two equations are needed.

$$V = \frac{c}{\sqrt{\varepsilon}} \tag{A.1}$$

$$d = \frac{TWTT * V}{2} \tag{A.2}$$

Where V is the velocity (m/ns), c the speed of light, $\varepsilon$is the relative permittivity, $TWTT$ is the two way travel time (ns), and d is the depth (m). Equations source (Campbell, Affleck, and Sinclair, 2018). This is used by the computer program, ReflexW, which will be further introduced later. Velocities are on a normal basis estimated from standard values (e.g. table 2.1), but can also be measured with either measuring with the GPR over a reflector with a known depth or with a CMP-analysis. According to Murray, Booth, and Rippin, 2007, the velocity for GPR in the Tsanfleuron glacier is 0.1596 – 0.1650 m/ns.

Tunnels or holes in the sub surface present them self as hyperbolas on the radar profile, and this is due to how the signal travels below the surface. The first signal that hits the void is actually going sideways, but will be displayed as lying directly beneath the receiver which will be located at a further depth than it actually is. The closer the

TABLE A.1: Properties observed for different medium at 100 MHz. Table after Davis and Annan, 1989

Material	**Relative permittivity** ε_r	**Velocity** $V\ (m\ ns^{-}1)$	**Electrical conductivity** $\sigma\ (mS\ m^{-}1)$
Air	1	0.3	0
Fresh water	81	0.033	0.5
Ice (pure)	3 – 4	0.16	0.01
Sand (dry)	3 – 5	0.15	0.01
Sand (wet)	20 – 30	0.6	0.01 – 1

transmitter/receiver gets to the void, the more accurate in depth will the display be, to be the shortest right on top and then again increase as the transmitter/receiver moves further away from the void. See figure A.1 for visualisation.

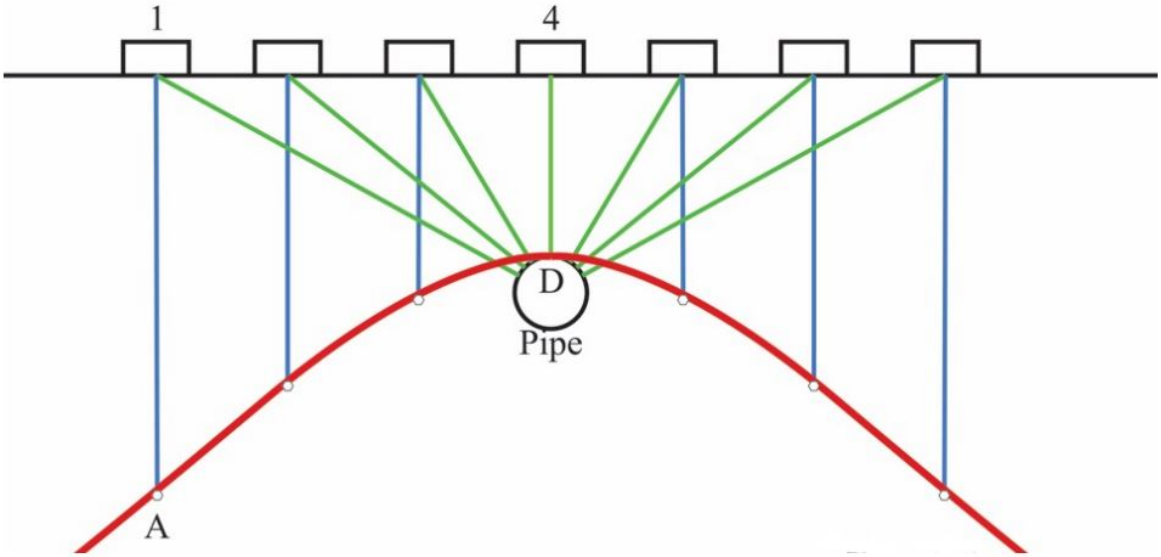

FIGURE A.1: How a hyperbola forms from a void or an item in GPR data. Figure courtesy by Professor Erik Sturkell.

A.2 CMP

To find a suitable velocity for the ice, a CMP had to be done. CMP-surveys are not done on a normal basis, since standard velocities tend to be most commonly used. This is easier, but yields a result that is not as accurate. Doing a CMP-analysis makes the results more accurate, as it is based on a velocity calculated for the specific location

and material. Here it will also be used for validations of the velocities calculated from the ice tunnel at Langjökull.

The CMP-method is used to determine the wave-velocity in a medium where it is not known. For this study, the velocity for glacial ice was just estimated to 0.18 m/ns in the beginning, as a denser form of ice, but to be able to make a true estimation of the ice thickness, a new velocity had to be found (Jacob and Urban, 2016).

A CMP setup (see figure **??**) consists of the GPR-system and two antennas - the transmitting antenna, Tx, and the recieving antenna, Rx. Initially, they are separated with a *Nyqvist interval sampling distance*, nx, which is derived from equation **??**, where K or ε_r is the relative permittivity of the host material, and f the antenna frequency (central operating frequency). In short, the Nyqvist interval can be calculated as a quarter of the wavelength in the material of the host. For every sounding, the antennae are then separated with one nx in total, so each antenna is moved $0.5nx$ from the midpoint.

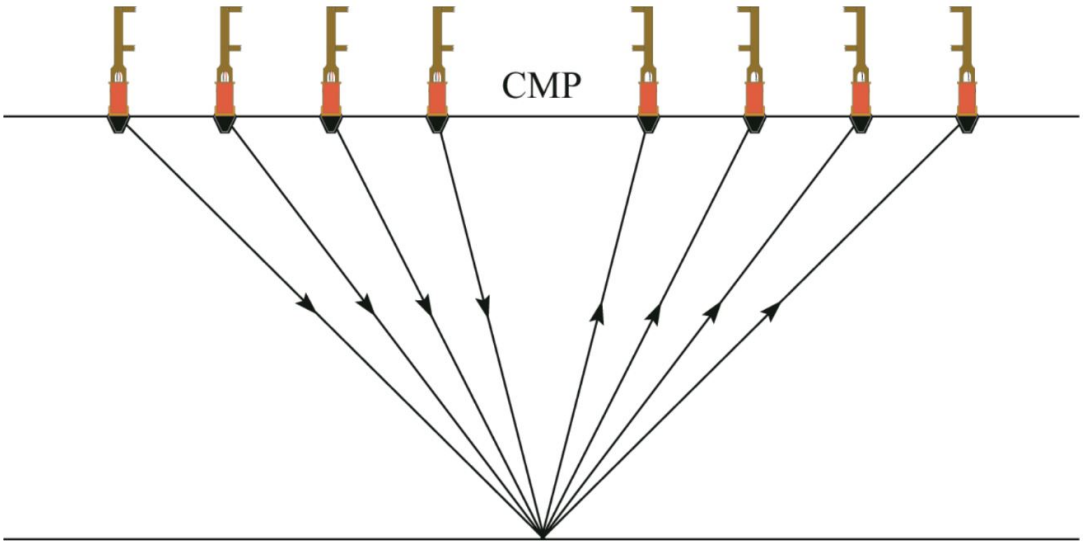

FIGURE A.2: CMP-setup that illustrates the moveout by Nx from a common mid point. Figure courtesy by Professor Erik Sturkell.

Possible error sources for the resulting RMS velocity are non-horisontal layers in the subsurface relative to the surface of the ground, how the antenna are positioned and how the signals are picked (Edward Barrett, Murray, and Clark, 2007).

$$n_x = \frac{c}{4f\sqrt{K}} = \frac{75}{f\sqrt{K}} \tag{A.3}$$

B Seismic Reflection Analyst Tutorial

By Christoffer Bergstrand and Jennifer Johansson, written as an Appendix to their report in the course Marine Geophysics in 2013.

Seismic Reflection Analyst Tutorial

Written by Christoffer Bergstrand & Jennifer Johansson

Part 1: Coordinate processing.

1. The coordinates that you have received for the profiles is in SWEREF 99 TM.
2. Convert the coordinates into WGS 84.
   i. Use this link: http://rl.se/rt90.

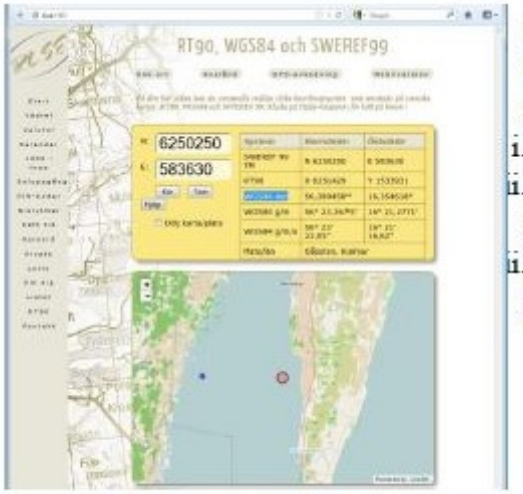

3. Calculate the lengths of all the profiles together with the distance between the first profile to the other profiles.
   i. Be sure to use dot instead of comma.
   ii. Latitude is the north value and longitude is the east value.
   ii. Use this link: http://seismo.cqu.edu.au/CQSRG/VDistance/.

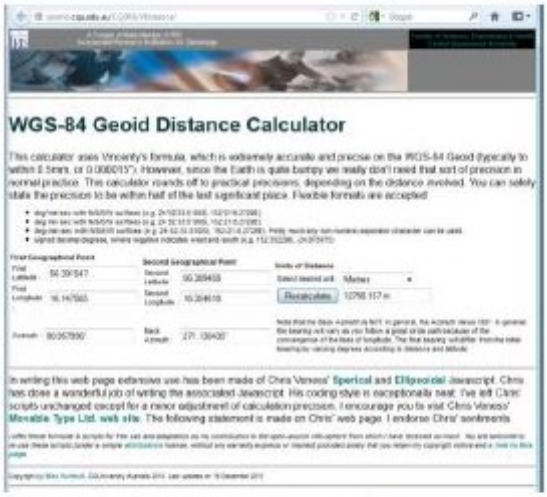

Part 2: Calculating the X and Y scale values for the different profiles.

1. Print out the seismic profiles on to A3 papers.
2. The profiles lengths are calculated in Part 1.
3. For the depth values you have to measure the distance in cm between the 0 m and 80 m depth indicators in order to find out what 1 cm on the paper is in reality. Then measure the distance between the 0 m indicator and the bottom continuous line, followed by multiplying this value with the meter-value equivalent to the 1 cm.
   i. Measure every profile because they most certainly have different scales.
   ii. You do this in order to know the depth and length between 4 marked corners in the profiles images for the georeferencings carried out in Part 3.

Part 3: Plotting of seismic reflections.

1. Open **ArcCatalog** and connect the folder that you want to work in by clicking on **Connect Folder**.
2. Create a **File Geodatabase** in your folder.

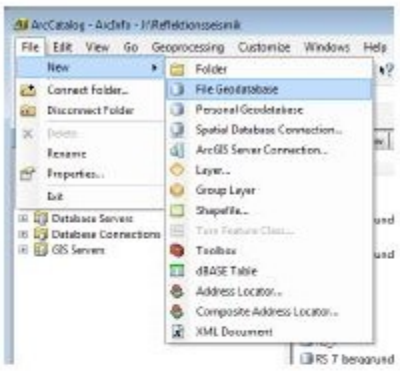

3. Open **ArcMap** and select **New map**.
4. Select your newly created geodatabase as default geodatabase before clicking **OK**.

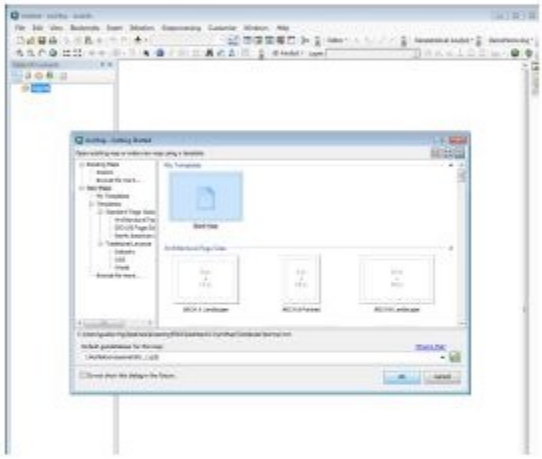

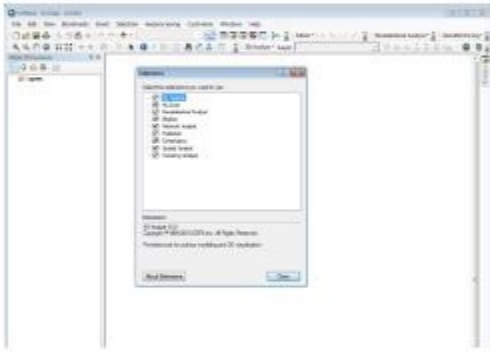

5. Click on **Customize** and then on **Extensions**.
6. Check all the empty boxes and click on **Close**.
7. Under the **Table of Contents**, rename your layer **(Layers)** to something that refers to one of the profiles, for example Sp1.
8. Right-click on Sp1 and click **Properties**, under the tab **Coordinate System** click on the "+" in front of the folder **Predefined**, followed by **Projected Coordinate Systems**, **National Grids** and **Sweden**.

9. Select the coordinate system **SWEREF 99 TM**.

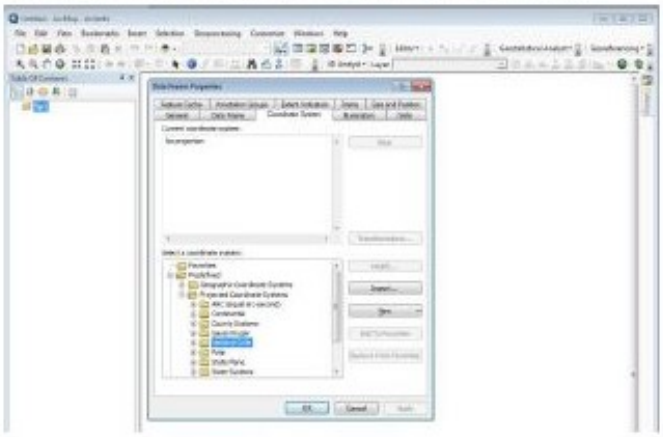

10. Go to your folder with the profile images and drag across one image, for example Ksd10_001_sp, and release it at your layer (Sp1).
11. Press **Yes** when prompted to create pyramids.
12. Make the toolbar **Georeferencing** available.
13. Click on the symbol for **Add Control Points**.

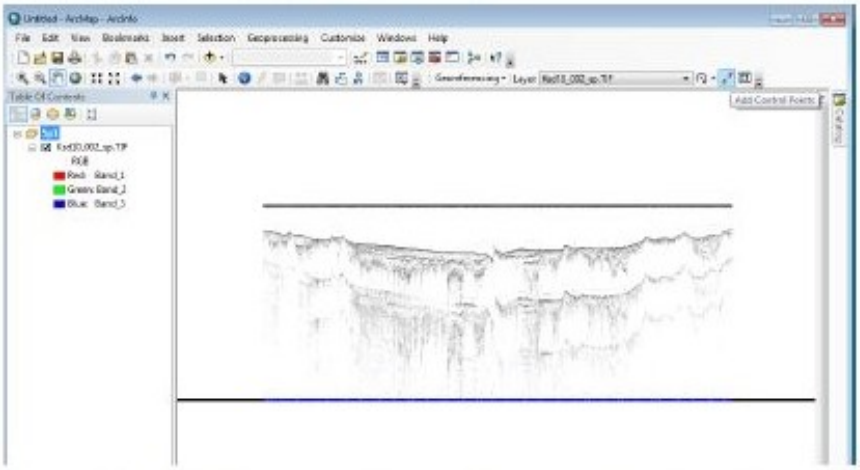

14. Zoom in on the left side of the profile, for example at the edge of the water surface.
15. Press once with the left and then once with the right mouse button on the selected corner without moving the mouse.
16. Select **Input X and Y** and write 0 for X and 0 for Y if it is for the left corner.
17. Do the same for the other corner at the water surface, but change the X value to the length of the profile.
18. 2 additional points need to be added to the two bottom corners, where Y should be in minus in order to show depths below the water surface.
    i. The scale should be corrected between X and Y to get a work-friendly depth, change the profile depth by multiplying Y values with, for example, 70. Do not forget to change back the values later in the exported excel-file.
19. Click on **Georeferencing** and select **Rectify**, save the file in your geodatabase with a descriptive name in order to avoid future problems.

20. Click on **View Link Table** and select **Save**, save the file in your folder with a descriptive name.

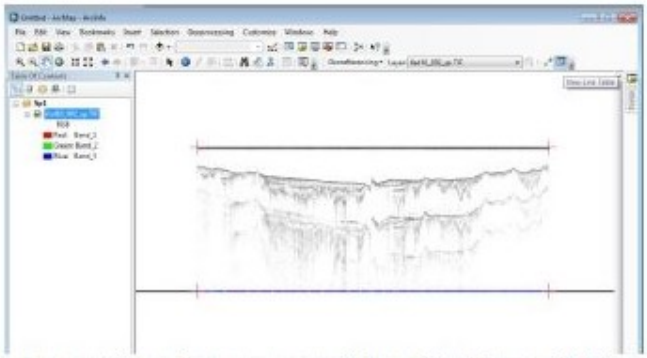

21. Open **ArcCatalog** again and create several shapefiles in your folder, one for every seismic layer that you want to plot. Use **Point** as Feature type.
22. Add one of the shapefiles to your layer (Sp1) in **ArcMap** by clicking at **Add Data**.
23. Make the toolbar **Editor** available.
24. Click on **Start Editing**.
25. If there are no templates under the **Create Feature** window to the right of the screen click on **Organize Templates**. In the new window that emerged click on **New Template** and then on Finish.
    i. If it is a template already available just click on it.
26. In ArcMap's lower right corner the **Construction Tools** is now available. Select **Points**.

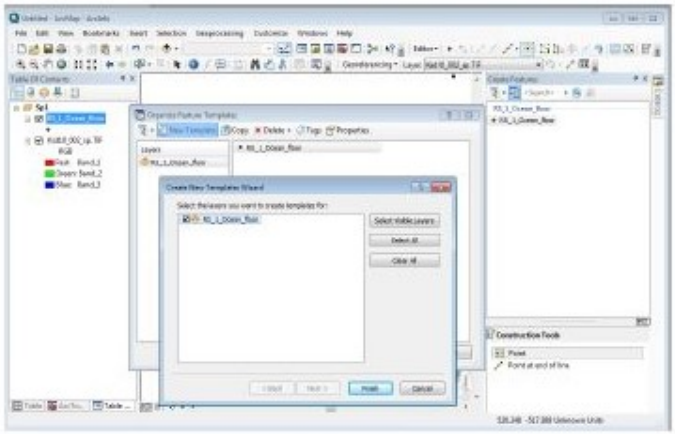

27. Zoom in to one end of the layer of interest, for example the ocean floor, and start to mark it with your left mouse button.
    i. Place the points as close together as possible in order to end up with an as detailed layer as possible.
    ii. Mark on the upper part of the layer.
    iii. Do not mark where you are unsure of the layer positioning.
28. When the entire layer has been mapped select **Save Edits** and **Stop Editing** in the **Editor** Toolbar.

29. Open **Attribute table** for the shapefile you just worked with.
30. Click on **Table Options** and select **Add Field**.
    i. Create one field for X and another field for Y.

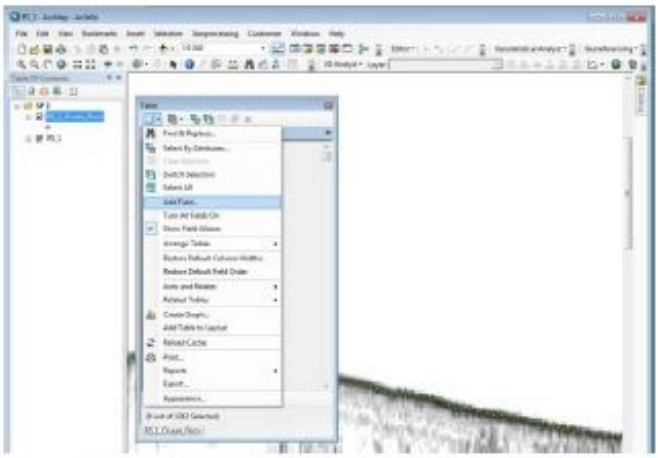

31. Choose **Select All.**
32. Right-click on X and select **Calculate Geometry**.
33. Choose **X Coordinate of Point** and click OK.
34. Right-click on Y and select **Calculate Geometry**.
35. Choose **Y Coordinate of Point** and click OK.
    i. Y should consist only of negative values as long as nothing is above the water surface.
36. Open **Excel** and write which layer you have recreated as well as X and Y in each column.
37. Now back in **ArcMap**, mark all the values in the attribute table, right click in the sidebar and select **Copy Selected**.
38. Paste all the values in Excel and remove the unnecessary data, keep only the values for X and Y.
39. Recalculate the Y values in order to get the correct depth values back from the multiplication done earlier.

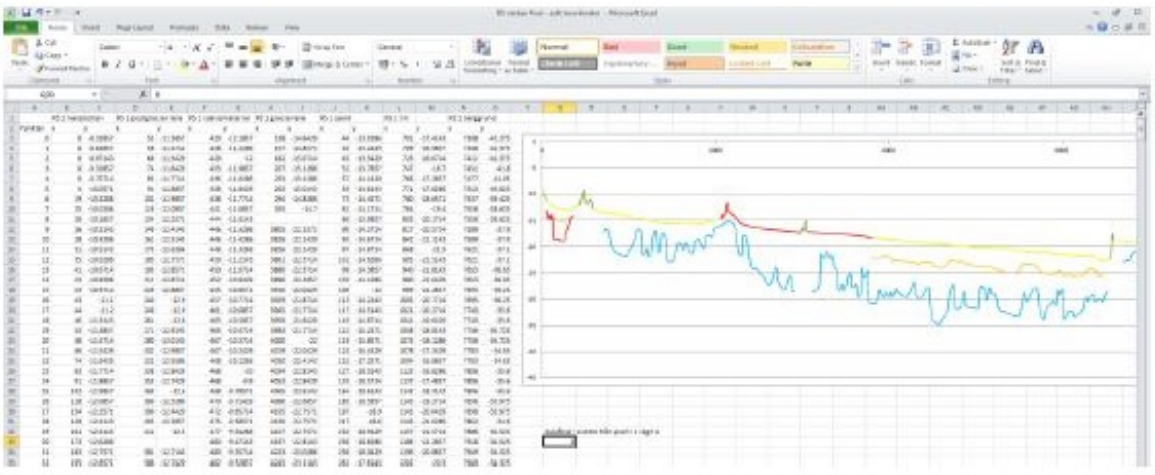

40. **Pay attention** to when you copy values from the Attribute table, you might not get the whole values, if the columns are too narrow. When this happens make the columns

wider and click on **Start Editing** again, before doing the recalculation of the X and Y geometry, in order to get the whole values. After copying the values again you may choose **Save Edits** and **Stop Editing**.

41. Repeat this steps until you have X and Y values for all the layers in a seismic profile.
42. **Create a graph** in excel showing the different layers in the profile, in order to detect possible errors in the data.
    i. When there are breaks in a layer from your analysis, you should create gaps in the X and Y values in order to recreate these breaks in your graph.
43. Now redo these steps for all the seismic profiles, with different geodatabases and different maps for all the profiles.
44. For the bedrock layers you have to use the image-files with the name "migr" instead of "sp". For the scale in depth you may have to use a different value to multiply with, for example 40 instead of 70, as done in step 18.
45. Use this excel-file as your original and create a copy of this one where you use the left corner of profile 1 as your starting point and then change all the X values in all the other profiles so that all the layers in the profiles are in the correct distance from the starting point of profile 1, in an east-west direction.
    i. You do this in order to get all the layers of the profiles in the right positions for the interpolations further on in part 4.

Part 4: Interpolate the layers.

1. Create a new Excel-file for every layer with X, Y and Z columns, where the same layer from all the profiles is plotted consecutively with no gaps in the rows.
    i. Values for X remains as X
    ii. Values for Y is changed to Z
    iii. The new Y is the distance between profile 1 and the profile of interest.

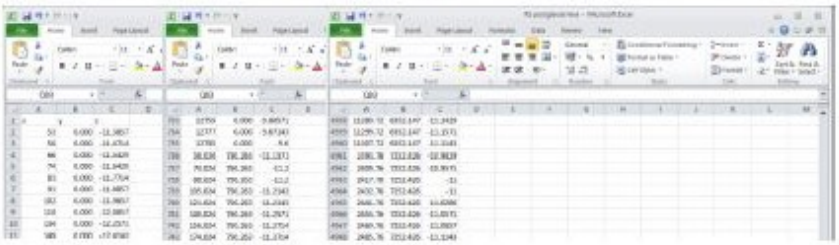

2. Create a new **File geodatabase** in ArcCatalog.
3. Open **ArcMap** and select **New map**.
4. Select your newly created geodatabase as default geodatabase before clicking **OK**.
5. Select **File**, **Add Data** and **Add XY Data**.

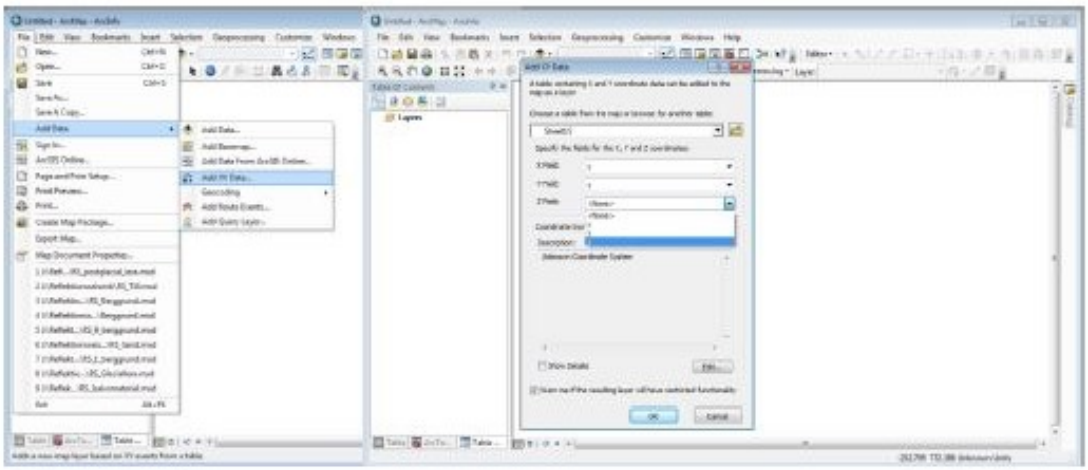

6. Select any of the excel-files and input the right letter for the right field.
7. Right-click on the added file in the **Table of Contents** and click **Data** followed by **Export Data**. Click **OK**.
8. Click on **Customize** and then on **Extensions**.
9. Check all the empty boxes and click on Close.
10. Open **ArcToolbox**, expand **Spatial Analyst Tools** and **Interpolation**.
11. Double-click on **IDW**.

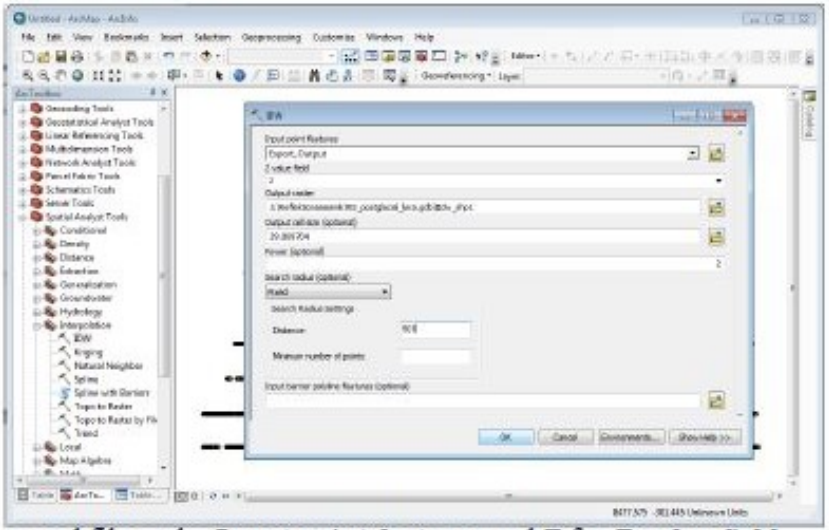

12. Select the exported file under **Input point features** and Z for **Z value field**.

13. Under **Search radius** select **Fixed** and under **Distance** write 901. This is the longest distance between two profiles.
14. Open **ArcCatalog** and create a shapefile.
15. Select **Polygon** instead of Point under **Feature Type**.
16. Add this polygon via **Add Data**.
17. In the toolbar **Editor** click on **Start Editing** and select the polygon-file.
18. Draw over the interpolated areas that you want to keep.
    i. Use different tools to achieve desired results.

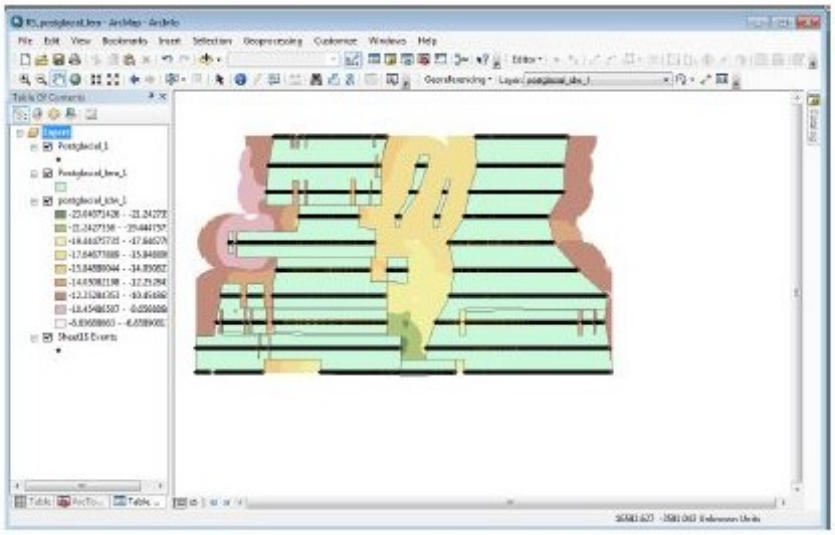

19. When all areas for one layer have been painted over select **Save Edits** and **Stop Editing**.
20. Open **ArcToolbox**, expand **Spatial Analyst Tools** and **Extraction**.
21. Double-click on **Extract by Mask** and run it after putting in the interpolated file as well as the polygon mask.

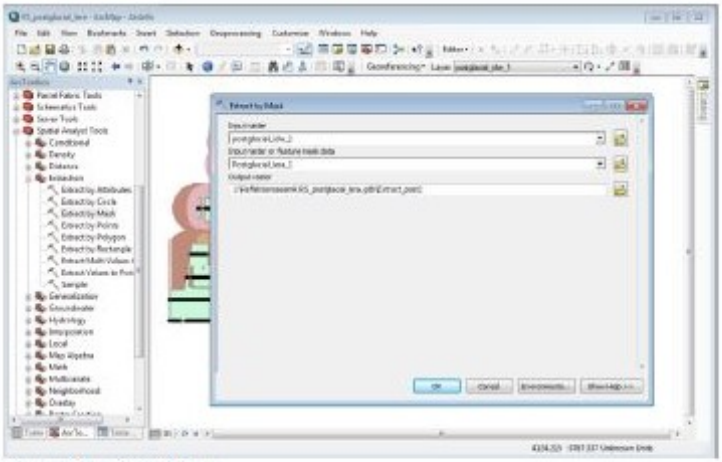

22. Save and close the **ArcMap**.
23. Do these steps for every layer.
24. Create a new **File geodatabase** in ArcCatalog.
25. Open **ArcScene** and select **New map**.
26. Select your newly created geodatabase as default geodatabase before clicking **OK**.

27. Click on **Add data** and select your masked interpolation-files, which should be in their geodatabase.
28. Right-click on each file under the **Table of Contents** and select **Properties**.

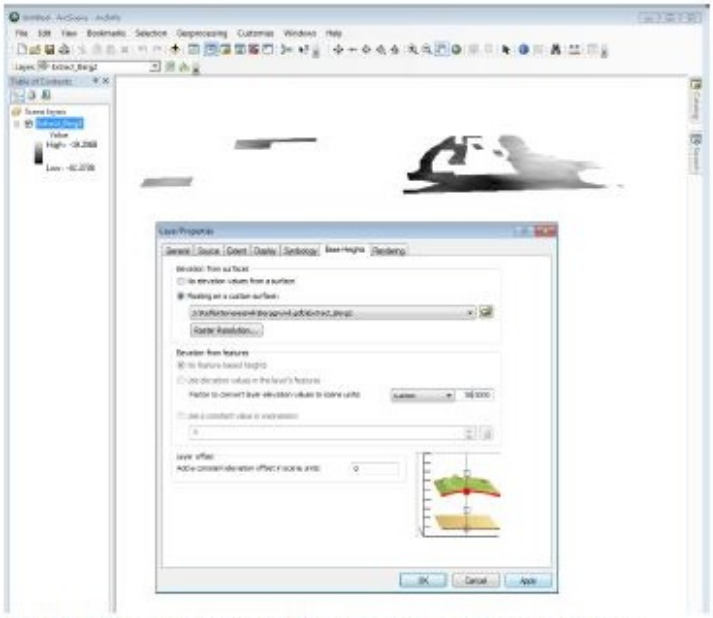

29. Select **Base Heights** and click in **Floating on a custom surface**.
30. Under **Elevation from features** you can put in any value, for example 30, to get altitude.

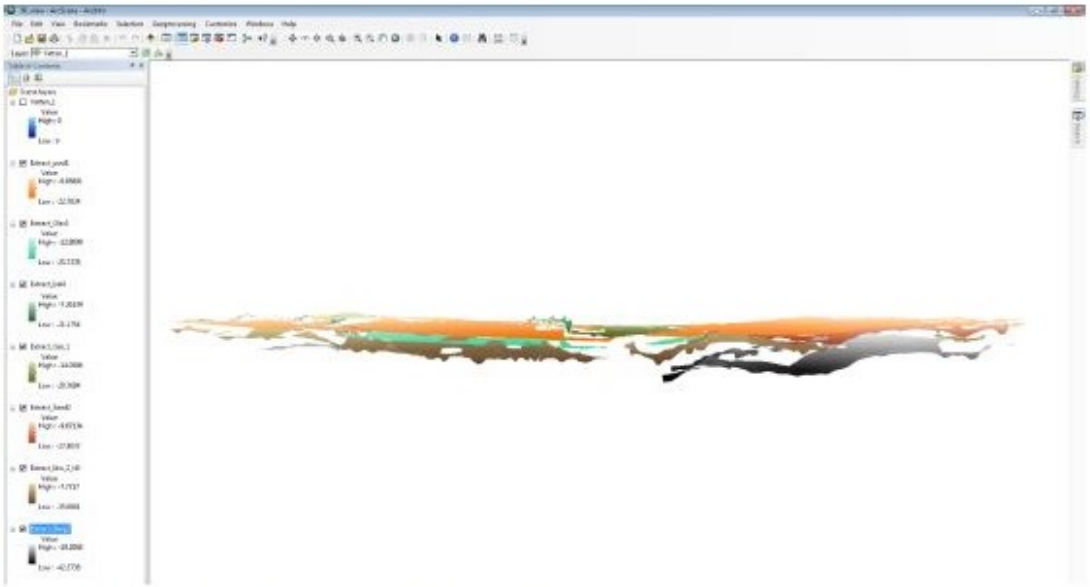

31. Select the appropriate colors for the layers.

Part 5: Create contours.

1. Open **ArcMap** for one of the interpolated layers.
2. Click on **Customize** and then on **Extensions**.

3. Check all the empty boxes and click on Close.
4. Open the tool **Contour** under **3D Analyst Tools** and **Raster surface** in **ArcToolbox**.

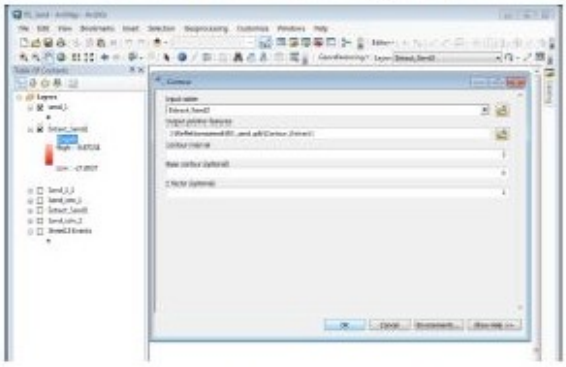

5. Select your masked interpolated layer under **Input raster**.
6. Choose the contour interval, for example 1 or 2.
7. Right-click on the newly created contour-file and select **Properties**.
8. In the tab **Symbology**, expand **Quantities** and **Graduated colors**.
9. Under **Field value** select **Contour**.

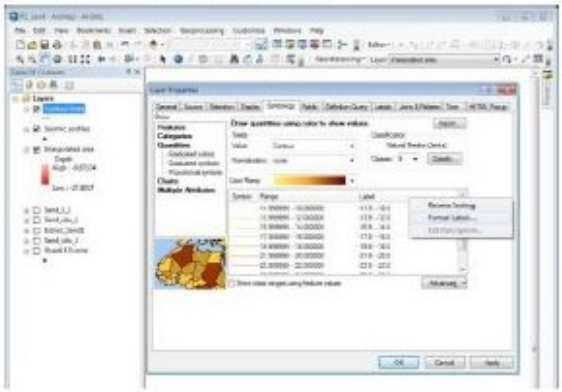

10. Under **Classification** and **Classes** choose a value for the number of meters that the layer lies within.
    i. You can do this in order to give every contour interval an individual color shade.
11. Select a contour color under **Color Ramp**.
12. Click on the tab **Labels**.
13. Check in the box **Label features in this layer**.
14. Under **Label Field** select **Contour**.

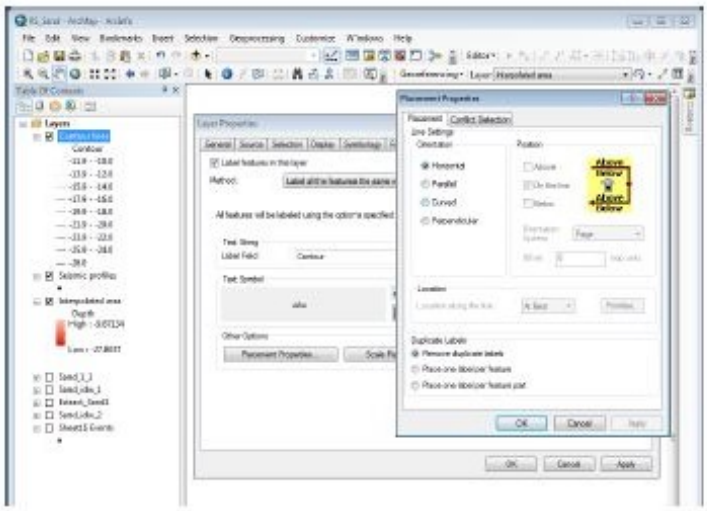

15. In **Placement Properties** different properties can be selected in order to change appearance and positioning of depth values.
16. Redo these steps for every layer.Part 6: Exporting layers.

1. Click on **View** and **Layout View**.
2. If you want to change the orientation of the paper you go to **Page and Print Setup** and select **Landscape**.
    i. This is also were you change paper size.

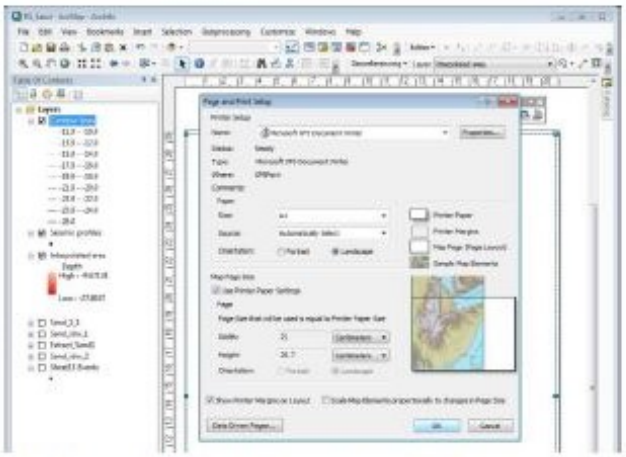

3. Change the shape of the dotted box to match the shape of the paper.

4. To zoom in on the object inside the page area select **Zoom In** from the toolbar **Tools** and not from the toolbar Layout.

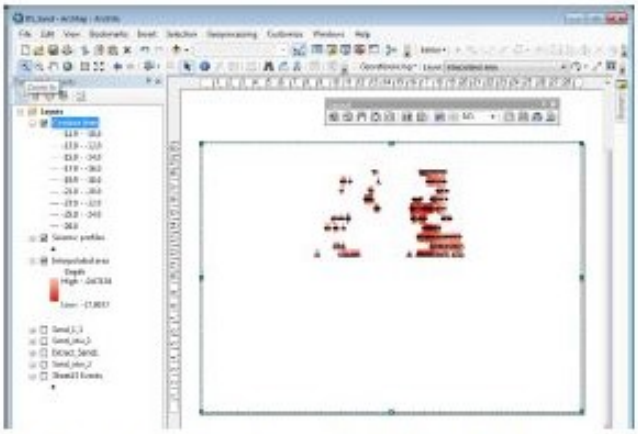

5. Move the object with **Pan** from the toolbar **Tools**.
6. Create a **Legend** located under **Insert**.
7. Click several times on **Next** and then on **Finish**.
8. Create a **Title** located under **Insert**.
9. Create a **North Arrow** located under **Insert**.
10. Click on **File** and **Export Map**.
11. Change the **Resolution** value to 720.
12. Select your folder and click **Save**.
13. Redo these steps for every layer.